



HAL
open science

Compensatory uptake functions in empirical macroscopic root water uptake models: experimental and numerical analysis

R. Albasha, J.C. Mailhol, B. Cheviron

► **To cite this version:**

R. Albasha, J.C. Mailhol, B. Cheviron. Compensatory uptake functions in empirical macroscopic root water uptake models: experimental and numerical analysis. *Agricultural Water Management*, 2015, 155, pp.22-39. 10.1016/j.agwat.2015.03.010 . hal-01541308

HAL Id: hal-01541308

<https://hal.science/hal-01541308>

Submitted on 19 Jun 2017

HAL is a multi-disciplinary open access archive for the deposit and dissemination of scientific research documents, whether they are published or not. The documents may come from teaching and research institutions in France or abroad, or from public or private research centers.

L'archive ouverte pluridisciplinaire **HAL**, est destinée au dépôt et à la diffusion de documents scientifiques de niveau recherche, publiés ou non, émanant des établissements d'enseignement et de recherche français ou étrangers, des laboratoires publics ou privés.

1 Compensatory uptake functions in empirical macroscopic 2 root water uptake models - Experimental and numerical 3 analysis

Rami ALBASHA ^{a b 1}, Jean-Claude MAILHOL ^a, Bruno CHEVIRON ^a

^a National Research Institute of Science and Technology for Environment and Agriculture

(Irstea), UMR G-eau, 361 Jean-François Breton street, 34136 Montpellier, France.

^b Department of Water Sciences, faculty of Civil Engineering, University of Aleppo, Ibn-

Albitar street, Aleppo, Syria.

4

5 **Abstract:** Macroscopic empirical root water uptake (RWU) models are often used in hydrological studies to
6 predict water dynamics through the soil-plant-atmosphere continuum. RWU in
7 macroscopic models is highly dependent on root density distribution (RDD). Therefore,
8 compensatory uptake mechanisms are being increasingly considered to remedy this
9 weakness. A common formulation of compensatory functions is to relate compensatory
10 uptake rate to the plant water-stress status. This paper examines the efficiency of such
11 compensatory functions to reduce the sensitivity of simulated actual transpiration (T_a),
12 drainage ($Drain_a$) and RWU patterns to RDD. The possibility to replace the compensatory
13 RWU functions by an adequate description of RDD is also discussed. The study was based
14 on experimental and numerical analysis of 2-dimensional soil-water dynamics of 11 maize
15 plots, irrigated using sprinkler (Asp), subsurface drip (SDI) systems, or rainfed (RF). Soil
16 water dynamics were simulated using a physically-based soil-water flow model coupled to
17 a macroscopic empirical compensatory RWU model. For each plot, simulation scenarios
18 involved crossing 6 RDD profiles with 6 compensatory levels. RDD was found to be the
19 main factor in the determination of RWU patterns, T_a and $Drain_a$ rates, with and without
20 the compensatory mechanism. The use of a water-tracking RDD, i.e., higher uptake
21 intensity in expected wetter soil regions, was found a surrogate for compensatory RWU
22 functions in surface-watering simulations (Asp and RF). However, in SDI simulations, a
23 water-tracking RDD should be combined to a high level of compensatory uptake to
24 satisfactorily reproduce real RWU patterns. Our results further suggest that the

11 Corresponding author. Tel: +33 4 67166323E-mail address: rami.albasha@irstea.fr (R.

2ALBASHA)

3

4

5

25 compensatory RWU process is independent of the plant stress status and should be seen
26 as a response to heterogeneous soil-water distribution. Our results contribute to the
27 identification of optimum parameterization of empirical RWU models as a function of
28 watering methods.

29**Key words:** Empirical macroscopic root water uptake models; Compensatory root water uptake;
30 Sprinkler Irrigation; Subsurface drip irrigation.

311. Introduction

32 Water uptake by plant roots is a key element in the process of water transfer in
33the soil-plant-atmosphere continuum ([Feddes et al., 2001](#)). In croplands, it is estimated
34that 65% of the precipitation is returned to the atmosphere by evapotranspiration ([Oki](#)
35and [Kanae, 2006](#)). Hence, pertinent simulation of the root water uptake (RWU) process
36is of major importance for an efficient agricultural water management. However, the
37RWU process is complex, related to endogenous factors (i.e., genetic control), and to
38exogenous factors such as soil water content, nutrient content, temperature, aeration
39and microbial activity (e.g. [Kramer and Boyer, 1995](#); [Hodge et al., 2009](#)).

40 Early experimental research to understand root behavior dates back to the end of
41the XIXth century, credited to the pioneer works of Charles and Francis Darwin (*The*
42*Power of Movement in Plants*, ([Darwin, 1880](#)), as has recently been recalled by [Baluska](#)
43et al. ([2009](#)). However, the first mathematical representations of RWU were
44undertaken some decades later by [van den Honert \(1948\)](#). Since then, RWU modeling
45is typically performed according to one of two approaches: the so-called microscopic
46and macroscopic approaches (e.g. [Molz, 1981](#); [Hopmans and Bristow, 2002](#); [Feddes](#)
47and [Raats, 2004](#)).

48 The microscopic models are physically-based. They consider water potential of
49both the root system and the soil in the immediate vicinity of roots, and describe thus
50water flow to and through individual roots analogously to Ohm's law. In contrast, the
51macroscopic approaches consider a lumped representation of both the roots and the
52soil. Although physically-based macroscopic RWU models exist in literature, which

53 consider root water potential (e.g., Heinen, 2001; de Jong van Lier et al., 2008;
54 Schneider et al., 2010; Couvreur et al., 2012), the macroscopic RWU models used in
55 literature are typically empirical, neglecting the hydraulic properties of roots (e.g.,
56 Feddes et al., 1978; van Genuchten, 1987).

57 The choice of one modeling approach instead of another is context-dependent
58 and still subject to debate (de Willigen et al., 2012): although physically based models
59 are insightful for the comprehension of water and nutrient uptake processes at the
60 root scale (Raats, 2007; Subbaiah, 2011) and require less calibration (Homaei et al.,
61 2002), their use is still limited in the domain of crop management due to the rich
62 parameterization and computational requirements of such models (Feddes and Raats,
63 2004; Subbaiah, 2011), compared to the less demanding empirical macroscopic
64 models (Feddes and Raats, 2004; Raats, 2007; Subbaiah, 2011), designated as more
65 “Hydrologically-oriented” (Feddes and Raats, 2004).

66 When integrated in a greater physically-based soil water transfer model, the
67 macroscopic RWU models conceptualize RWU by a sink term in the Richards equation:

$$68 \quad \partial\theta/\partial t = \nabla[k(h)\nabla H] - S \quad (1)$$

69 where θ denotes the volumetric soil water content [L^3L^{-3}], t the time [T], h the soil
70 pressure head [L], H the soil total head [L], k the hydraulic conductivity of the soil [$L T^{-1}$
71 L^{-1}] and S the sink term representing RWU [$L^3L^{-3}T^{-1}$]. The sink term S represents herein
72 the actual RWU, associating the potential transpiration (T_p) to a potential root uptake
73 distribution function (β) and to an uptake reduction function (γ) in a product formula:

$$74 \quad S = T_p \gamma \beta \quad (2)$$

75 The function β is typically taken in literature as the bulk root density distribution
76 (Hopmans and Bristow, 2002), and will be considered as such in this study.

77 Due to their simplifying assumptions, the empirical models have often been said
78 to have little biophysical basis (Skaggs et al., 2006, Javaux et al., 2008, Schneider et
79 al., 2010). Probably, the most important shortcoming in this type of model is the

80 assumption that root activity is proportional to root density and to local water-content
81 status through the aforementioned product formula. When described as such, RWU is
82 represented as a passive process, i.e. uptake rates are controlled solely by climatic
83 demand, the spatial distribution of soil water availability and root density.

84 In fact, it has been shown experimentally and numerically that the spatial
85 distribution of instantaneous RWU rates may differ strongly from that of root density
86 (Bruckler et al., 2004; Hodge, 2004, Faria et al., 2010). Such differences are expected
87 to be greater in heterogeneous soil structures (Kuhlmann et al., 2012) and to further
88 increase with time (Schneider et al., 2010). In addition, it has widely been shown
89 experimentally that plants adjust their water uptake patterns to cope with soil water
90 content distribution by an enhanced “compensatory” uptake from wetter soil regions
91 (e.g., Green and Clothier, 1995; Hodge, 2004; Leib et al., 2006). Skaggs et al. (2006)
92 suggested that the compensatory RWU mechanism plays a major role in simulations of
93 soil water transfer where irrigation methods impose non-uniform water deficits in the
94 root zone. Moreover, Kuhlmann et al. (2012) suggested that omitting the
95 compensatory uptake may lead to underestimate plant transpiration in heterogeneous
96 soils.

97 Attempts to conceptualize compensatory RWU in the empirical macroscopic
98 models were first undertaken by Jarvis (1989) who explicitly considered a
99 compensatory RWU function, multiplied by both γ and β functions. The author related
100 the compensatory uptake mechanism to the plant stress index, expressed by the ratio
101 of the actual to potential transpiration (T_a/T_p). Compensatory uptake is thus triggered
102 in a manner that transpiration is maintained at its potential level as long as T_a/T_p is
103 greater than a predefined threshold (ω_c). Pang and Letey (1998) also explicitly
104 accounted for the compensatory RWU, where plant transpiration is maintained at its
105 potential level as long as there is at least one soil region where water content is
106 greater than a given stress threshold.

107 Other compensatory RWU models in literature do not involve the T_a/T_p ratio
108 threshold, i.e., continuous. [Bouten et al. \(1992\)](#), [Lai and Katul. \(2000\)](#) and [Li et al.](#)
109 [\(2001\)](#) proposed that water uptake is proportional to both β and a weighted stress
110 index relating the local (considered soil element) to the bulk average (entire root zone)
111 water condition, regardless of the ratio T_a/T_p . [Adiku et al. \(2000\)](#) and [van Wijk and](#)
112 [Bouten \(2001\)](#) considered that RWU pattern from the soil is automatically adjusted to
113 minimize energy expenditure by the plant. Finally, water-tracking RWU models ([Coelho](#)
114 [and Or, 1996; 1999](#)), which attribute higher uptake intensity to wetter soil regions,
115 may provide an alternative method to implicitly account for the compensatory RWU
116 process as proposed by [Mailhol et al. \(2011\)](#). However, the latter method has not been
117 fully investigated in literature, and most studies account for the compensatory RWU
118 via explicit functions.

119 The Jarvis's explicit compensatory RWU function has lately been integrated in the
120 2-dimensional (2D) version of the water and heat transfer model in porous media
121 Hydrus ([Simunek et al., 2008](#)) as discussed by [Simunek and Hopmans \(2009\)](#). The
122 authors suggested that the effect of the spatial root distribution on RWU may be
123 reduced when compensatory RWU is considered, and concluded thus that a priori
124 knowledge of the spatial root distribution may only be effective for non compensatory
125 RWU simulations.

126 Despite all the attention, the Jarvis's function is perceived oversimplifying
127 compared to microscopic modeling approach ([Schneider et al., 2010; Javaux et al.,](#)
128 [2013](#)). Moreover, few information exists in literature on the values the ω_c threshold
129 one should take ([Skaggs et al., 2006](#)), which often leads to use of arbitrary values
130 ([Shouse et al., 2011](#)) or, in some cases, to abandon the use of the compensatory
131 function ([Oster et al., 2012](#)).

132 Therefore, with such uncertainties in Jarvis's function parameterization, the effect
133 of the latter on RWU pattern as evoked by [Simunek and Hopmans \(2009\)](#) is
134 questionable, especially since root density distribution is well known to highly

135determine RWU pattern and rates (e.g., [Beudez et al., 2013](#)). One may wonder
136whether a compensatory RWU is even needed when an adequate description of root
137density is provided, e.g., with water-tracking RWU.

138 The aim of this study is to (i) examine the effects of the compensatory RWU
139function of [Jarvis \(1989\)](#), on both the rates of water outfluxes from the soil domain
140(transpiration and drainage) and the RWU pattern, when contrasted macroscopic root
141density profiles are used in combination with different compensatory levels; (ii)
142explore the possibility of the use of root density profiles specific to the watering
143method, water-tracking RWU models, as an approach to replace the need for
144compensatory uptake functions.

145 The model used for the numerical analysis is the well documented Hydrus
146(2D/3D) model ([Simunek et al., 2008](#)), which includes an adapted form of the
147[Jarvis \(1989\)](#) function. The simulations were performed to predict water flow in the soil
148for existing sprinkler-irrigated (Asp), subsurface drip-irrigated (SDI) and rainfed (RF)
149maize plots. The compensatory uptake levels (T_a/T_p) ranged from 1.0 (no
150compensatory uptake) to 0.5 (maximum compensatory level considered). Root profiles
151used were either hypothetical or obtained from *in-situ* root density observations. The
152hypothetical RDD profiles were presumed to correspond to the real root activity
153pattern depending of the watering method, as water-tracking RWU models.

1542. **Materials and Methods**

155 Field experiments were conducted to (i) characterize *in-situ* the spatial
156distribution of root density of irrigated maize, (ii) monitor its vegetative development,
157and (iii) monitor the temporal evolution of soil volumetric water content (θ) profiles.
158These data were needed as input and verification of the numerical analysis. The
159description of the field experiments and the numerical analysis procedures is given in
160the following sections.

161 **2.1. Field experiments**

162 The experiments were conducted at the Lavalette experimental station (43°40
163N,3°50 E) of the Irstea research institute (formerly Cemagref), in Montpellier, SE
164France. Lavalette is fully equipped with a meteorological station which provides rainfall
165and the reference crop evapotranspiration (ET_{ref}) according to [Penman \(1948\)](#). The
166meteorological station is situated at an average distance of 100 m from the
167experimental plots.

168 The experiments were conducted in 2008, 2011 and 2012 on maize plots which
169were either irrigated using SDI or Asp systems, or rainfed. The driplines of the SDI
170plots were buried at 35 cm depth, having an emitter spacing of 30 cm and a lateral
171dripline spacing of 160 cm. In all 3 years, SDI plots were irrigated at levels of 70-
17280%ETM whereas the Asp plots were irrigated at levels of 70%ETM in 2008 and 100
173and 50%ETM in each of 2011 and 2012.

174 All measurements were taken within defined sub-plots of a small surface (5*5 m²)
175situated in the center of each experimental plot (1200 m²) in order to eliminate border
176effects. Rain or sprinkler water influxes were measured by rain gauges situated next to
177the measurement sites. Similarly all fertilizer quantities were also controlled over the
178surface of the measurement plots.

179 **2.1.1. Agronomic practices and measurements**

180 The agronomic practices were similar in all 3 years. A dent hybrid maize variety
181was used in all three years of experiments (Pioneer PR33TY65 in 2008 and PR34P88 in
1822011 and 2012). Sowing took place on day of year (DOY) 120 in 2008 and on DOY 110
183in both years 2011 and 2012. Sowing lines were spaced by 80 cm and were directed
184East-West, aligned to SDI driplines.

185 The distance between the sowing lines and the driplines varied for each season
186within each measurement subplot. This distance was equal to 40, 30 and 65 cm
187respectively in 2008, 2011 and 2012.

188 Crop water requirements were estimated based on the crop maximum
189 evapotranspiration (ETM) approach (Allen et al., 1998). ETM was estimated on a daily
190 basis as a function of ET_{ref} (provided by the meteorological station) and the crop
191 coefficient (K_c) which is calculated as a function of the simulated Leaf Area Index (LAI)
192 according to Allison et al. (1993). ETM served as a base point to estimate irrigation
193 requirements after subtracting rainfall quantities. The total applied water replaced the
194 full or a fraction of ETM depending on the predefined stress levels for each treatment.
195 Cumulative rainfall and irrigation quantities are given in Figure 1.

196 The cumulative rainfall during the three growing seasons 2008, 2011 and 2012
197 totaled 233, 179 and 236 mm, respectively. Total irrigation amounts were 325 and
198 335 mm for fully-irrigated Asp treatments and 117 and 143 mm for the severely-
199 stressed Asp treatments respectively in 2011 and 2012, while the mild-stressed Asp
200 treatment received 260 mm in 2008. Finally, SDI plots were supplied by 235, 240 and
201 268 mm in 2008, 2011 and 2012, respectively.

202

203 *Figure 1: Cumulative rainfall and irrigation quantities applied to all plots during the growing*
204 *seasons 2008, 2011 and 2012.*

205

206 The applied quantities of nitrogen fertilizers for post emergence were calculated
207 based on the soil N content at the sowing date, the soil mineralization rate (0.8 kg ha^{-1}
208 d^{-1}) during the crop cycle and the expected yield so that total N amounts were not a
209 limiting factor for crop growth and grain production.

210

211 In each of the measurement plots, the vegetative development of maize was
212 monitored regularly by measurements of the LAI, using LI-COR LAI-2000 Plant Canopy
213 Analyzer LAI-meter. The measurements were performed at 5 locations in and around
214 the measurement plots, and the mean values were then taken.

215 The estimation of θ was performed using the neutron scattering method (CPN
216503 DR, Campbell Pacific Nuclear Corp., Concord, CA, USA). The neutron probe was
217calibrated based on gravimetric soil water content and bulk density measurements
218performed on soil samples collected prior to each crop cycle from 4 soil layers (0-30,
21930-60, 60-90 and 90-120 cm). Probe-access tubes were installed vertically in a maize
220row in each measurement plot. Some plots had an additional tube installed at mid-
221distance between two crop rows. Measurements were taken in most cases to a
222maximum depth of 200 cm, at 10 cm interval.

223 Further information in agronomic practices may be found in ([Mubarak et al.,](#)
224[2009a,b](#)) and ([Mailhol et al., 2011](#)).

225 **2.1.2. Root density observations**

226 The aim of the *in-situ* characterization of root density was to (i) show
227experimentally whether the spatial distribution of root density (RDD) may be related to
228the watering method and (ii) to use the resulting RDD profiles in the numerical
229analysis.

230 Root density was characterized in 2008 and 2011 at the end of the maize cycle.
231The data collected in both years were further enriched by data collected by former
232similar works performed at the Lavalette station, available from its database. In all
233cases, the simple method of [Tardieu and Manichon, \(1986\)](#) was applied (e.g., [Mubarak](#)
234[et al., 2009a](#)). According to this method, soil pits (about 2.0 m long, 1.0 m wide and
2351.8 m deep) were excavated at the harvest of each experimental campaign,
236perpendicularly to the maize rows. The faces of the pits were vertical planes,
237subdivided in square cells (5*5 cm). Root density was assessed based on visual
238observation. A number ranging from 0 to 5 was assigned to each cell according to the
239visually observed density in a 1 cm layer of the exposed soil surface.

240 Figure 2 shows the observed RDD profiles for Asp (A, B and C) and SDI (D, E, F,
241and G) plots (only 4 SDI profiles are illustrated for the sake of visibility).

242 Figure 3A shows the mean vertical RDD (the means of each horizontal line) for
243 both irrigation methods, whereas the mean horizontal RDD (the means of each vertical
244 line) is shown in Figure 3B for Asp and Figure 3C for SDI plots.

245

246 *Figure 2: Observed root density profiles of Asp (A, B, C) and SDI (D, E, F, G) maize plots. The*
247 *driplines are presented by filled black circles. Root density was evaluated visually following*
248 *the method of Tardieu et al. (1986). The observed profiles come from different experimental*
249 *campaigns as denoted for each profile.*

250

251 *Figure 3: The mean horizontal root density distribution (A) for both Asp and SDI maize plots,*
252 *and the mean vertical root density of Asp (B) and SDI (C).*

253

254 Since the root profiles are reconstructed from visual observations, the density
255 indices are prone to the subjective evaluation made by the different observers and
256 therefore these data are rather qualitative.

257 Roots were found to occupy the entire soil domain under maize rows and in the
258 inter-row space, for both irrigation methods (Figure 2). Only a small decrease in root
259 density was observed as the horizontal distance from the crop row increases
260 (Figure 3B and C). Moreover, both Asp and SDI methods result in similar vertical RDD,
261 with slightly higher density values for Asp in the upper 40 cm soil layer (Figure 3A).
262 Furthermore, an interesting indication appears in Figure 2 for the SDI maize profiles:
263 root density seems independent of the irrigation method, since no systematic increase
264 in root density was observed in the vicinity of the drippers (represented by a blue
265 circle), even for the same plot (Figure 2E).

266 The aforementioned observations do not plead in favor of the use of RDD profiles
267 that are specific to a watering method. The results suggest that a 2D RDD profile
268 where the root density decreases linearly, in both vertical and horizontal directions,
269 adequately describes root systems (and consequently the potential RWU pattern) for
270 both Asp and SDI systems. This observed RDD profile, denoted β_{Obs} , was used in the

271 numerical analysis with 5 additional hypothetical RDD profiles as will be further
272 described in section 2.3.

273 2.2. Numerical analysis

274 2.2.1. Water flow simulation model

275 The Hydrus (2D/3D) model was used to simulate water flow in the soil by a
276 numerical solution to the Richards equation (Richards, 1931) supplemented with a
277 term S to account for root water uptake. To reduce the number of the spatial
278 dimensions from three to two, it is assumed that water flow occurs only in a vertical
279 plane perpendicular to the crop rows. This assumption stands for sprinkler irrigation as
280 long as water application is uniform over the soil surface in the row direction. For SDI,
281 it is assumed that water bulbs formed by the emitters overlap and merge forming a
282 continuous cylindrical wetted zone along the dripline rendering thus water flow a 2D
283 problem (Lafolie et al., 1989).

284 Considering the aforementioned assumptions and considering the soil to be
285 isotropic, the equation describing the flow in a vertical plane is:

$$286 \quad \frac{\partial \theta}{\partial t} = \frac{\partial}{\partial x} \left(\frac{k(h, z) \partial h}{\partial x} \right) + \frac{\partial}{\partial z} \left(\frac{k(h, z) \partial h}{\partial z} \right) - \partial k(h, z) / \partial z - S \quad (3)$$

287 where x and z are respectively the horizontal and vertical (positive upwards) Cartesian
288 coordinates [L]. The macroscopic RWU sink term S is given by:

$$289 \quad S = T_p \gamma(h) \beta(x, z) \phi \quad (4)$$

290 where T_p [L T⁻¹] is the potential transpiration, $\gamma(h)$ is the transpiration reduction
291 function [-], $\beta(x, z)$ is the potential RWU pattern which is identical to root density
292 distribution RDD [L L⁻²], and finally ϕ is the compensatory uptake function of Jarvis
293 (1989):

$$294 \quad \phi = \begin{cases} 1/\omega; & \omega \geq \omega_c \\ 1/\omega_c; & \omega < \omega_c \end{cases} \quad (5)$$

295 where ω is the plant stress index (T_a/T_p) and ω_c is a critical stress index threshold (see
 296 [Jarvis, 1989](#) and [Simunek and Hopmans, 2009](#) for details).

297 In the present study, the piece-wise stress-response reduction function of [Feddes](#)
 298 [et al. \(1978\)](#) was used:

$$299 \quad Y = \begin{cases} 0; & h \geq h_1 \\ (h_1 - h)/(h_1 - h_2); & h_1 > h \geq h_2 \\ 1; & h_2 > h \geq h_3 \\ (h - h_4)/(h_3 - h_4); & h_3 > h \geq h_4 \\ 0; & h_4 > h \end{cases} \quad (6)$$

300
 301 The values of h_2 and h_3 represent the thresholds between which water uptake is
 302 assumed maximum, while h_1 and h_4 represent respectively the thresholds of oxygen
 303 deficiency due to soil saturation and the minimum soil water content observed in the
 304 core of the root system (generally close to the wilting point). The values of h_1 , h_2 and
 305 h_4 were taken equal to -15, -30 and -15000 cm, respectively. [Feddes et al. \(1978\)](#)
 306 suggested that the value of h_3 depend on the transpiration rate. h_3 is therefore
 307 assumed to decrease as the transpiration rate decreases. Thus, h_3 was taken equal to
 308-325 and -600 cm for transpiration rates of 5 and 1 cm day⁻¹, respectively. The
 309 parameters values of the [Feddes et al. \(1978\)](#) function were fixed for all simulations.

310 Finally, the actual transpiration is calculated as the integral of S over the root
 311 zone (Ω_R):

$$312 \quad T_a = T_p \int_{\Omega_R} Y(h) \beta(x, z) \varphi d\Omega_R \quad (7)$$

313 The different normalized root density distribution functions $\beta(x, z)$ used in the present
 314 study will be detailed in subsection 2.3.

315 **2.2.2. Soil domain characteristics**

316 The width of the soil domain was set so that a zero horizontal flux Neuman-type
 317 boundary condition (BC) may be assumed across the lateral vertical boundary

318elements (Figure 4). The soil domain was thus centered over a crop row, and the soil
319surface width was taken equal to the spacing between two maize rows (80 cm) in Asp
320and RF plots. The width of SDI plots was taken equal to the half of the distance
321between two drip lines, assuming that a zero horizontal flux occurs on both verticals
322under the dripline, and at mid-distance between two driplines.

323

324 *Figure 4: The geometry and boundary conditions (BC's) imposed to the soil domains with*
325*dimensions given in cm. Γ_1 is a zero horizontal flux BC, Γ_2 is an atmospheric BC, Γ_3 is a constant*
326*water-content BC and Γ_4 is a variable flux BC. The horizontal pink line at 120 cm represents the*
327 *maximum root depth at which drainage was calculated.*

328 The depth of the soil domain was set so that a Dirichlet-type constant soil-water
329content BC may be considered at the lower soil boundary. The depth at which changes
330in the value of θ were negligible was approximately 190 cm for most treatments.
331Therefore, the maximum depth of the soil domain was set to 200 cm.

332 Finally, on the soil surface, an atmospheric variable fluxes BC was imposed. All
333atmospheric fluxes were assumed to be uniformly distributed over the soil surface.
334While daily rainfall fluxes were readily available from meteorological station records,
335the daily potential fluxes of crop transpiration T_p and soil evaporation E_p had to be
336calculated from the daily ETM, using an external crop model.

337 The Pilote model ([Mailhol., 1997](#); [Mailhol et al., 2011](#)) was used to separate ETM
338into T_p and E_p , as a function of the LAI according to [Ritchie \(1972\)](#) and [Novak \(1981\)](#).
339This model has been shown to yield good predictions of soil-water reserves, LAI and
340biomass production of maize crop in the pedo-climatic context of the Lavalette station,
341for surface irrigated plots, subsurface irrigated plots ([Mailhol et al., 2011](#)), both for
342tillage and no tillage practices ([Khaledian et al., 2009](#)). Pilote is a one dimensional
343bucket-type model. This model assumes the soil domain to be homogeneous and
344isotropic over the entire root zone, and the crop water use to be optimum as long as
345the lumped soil-water reserve of the root zone is greater or equal to the readily

346 available water. Therefore, T_p is root density-independent and the resulting T_p and
347 E_p fluxes of each plot may be used in Hydrus (2D/3D) simulations regardless of the β
348 profiles used.

349 Finally, the vertical soil profile of the Lavalette station shows 3 layers
350 distinguished with specific hydrodynamic properties. Mubarak et al. (2009a) fitted soil
351 hydrodynamic parameters to the van Genuchten-Mualem model (van Genuchten,
352 1980; Mualem, 1976), as described in Table 1.

353
354 *Table 1: The hydrodynamic parameters of the van Genuchten-Mualem model (van Genuchten,*
355 *1980; Mualem, 1976) model fitted to the soil of Lavalette station. θ_r and θ_s denote respectively*
356 *the residual and saturated volumetric soil water contents, α and n are empirical shape*
357 *parameters, K_s is the soil hydraulic conductivity at saturation and l is a pore connectivity*
358 *parameter.*

359

360 **2.3. Scenarios**

361 To summarize:

362 The Hydrus (2D/3D) model was run for the simulation of water flow in the soil of
363 11 treatments cultivated with maize:

364 • AspETM (11) and AspETM (12): sprinkler, fully-irrigated treatments in 2011 and
365 2012,

366 • Asp70ETM (08), Asp50ETM (11) and Asp50ETM (12): sprinkler, deficit-irrigated
367 treatments (30% deficit in 2008 and 50% deficit in both 2011 and 2012),

368 • SDI (08), SDI (11) and SDI (12): SDI, deficit-irrigated treatments (30% deficit in
369 all 3 years),

370 • RF (08), RF (11) and RF (12): rainfed treatments in 2008, 2011 and 2012.

371 For each of the 11 treatments, water flow was simulated for 36 scenarios (6 β
372 profiles and 6 ω_c levels). The levels of ω_c ranged from 0.5 (the maximum
373 compensatory uptake level considered) to 1.0 (non-compensatory uptake). The 6 β
374 profiles are illustrated in Figure 5:

375 1. The “observed” RDD profile (β_{obs}): root density decreases linearly in both the
376 vertical and horizontal directions, as discussed in [section 2.1.2](#).

377 2. The “sprinkler-specific” profile (β_{Asp}): root density decreases exponentially in
378 both the vertical and horizontal directions. This profile was constructed using the [Vrugt](#)
379 [et al. \(2001\)](#) function, implemented in the Hydrus (2D/3D) model. We hypothesize by
380 using this profile that root activity is mainly concentrated in the shallow soil layers
381 since irrigation is applied at the soil surface.

382 3. and 4. Two “SDI-specific” profiles, respectively $\beta_{\text{SDI-1}}$ and $\beta_{\text{SDI-2}}$: the maximum
383 root density is located in the vicinity of the dripper ($\beta_{\text{SDI-1}}$) or at the same depth of the
384 dripper on the vertical of the plant row ($\beta_{\text{SDI-2}}$). Those two profiles were selected to
385 correspond to match the cases where root density was observed to increase near the
386 drippers (Figure 2F, G). We hypothesize thus that uptake activity of the roots mainly
387 takes place at deeper layers as a response to the subsurface allocation of irrigation
388 water.

389 5. A constant root density profile (β_{Cst}): one may suggest that β_{Cst} represents an
390 average profile that may be used in the case where an *a-priori* knowledge of the real
391 root density is missing, as suggested by [Kandelous et al. \(2012\)](#).

392 6. Finally, a profile of increasing root density with depth (β_{Inc}) was added. β_{Inc} is
393 horizontally constant but increases linearly with depth. Although β_{Inc} is in total
394 contradiction with the observations of root systems of most biomes ([Schenk and](#)
395 [Jackson, 2002](#)), one may hypothesize that such profile may reflect an increase uptake

396 activity of deep roots as soil surface dries out (e.g., [Klepper, 1991](#)). The addition of
397 this profile aimed principally to maximize the contrast in the examined RDD profiles.

398 *Figure 5: Root density profiles of fully-developed maize irrigated with SDI with driplines located*
399 *on the right-side boundary at a depth of 40 cm. X^* and Z^* are the horizontal and vertical*
400 *coordinates at which the root density is maximum. X_{max} and Z_{max} delimit the soil region*
401 *occupied by roots. P_x and P_z are empirical shape parameters (specific to the function of [Vrugt](#)*
402 *[et al. \(2001\)](#)).*

403 The numerical scheme of the simulations for each of the 11 treatments is shown
404 in Figure 5. Since Hydrus (2D/3D) does not simulate the increase of root depth with
405 time, a series of simulations had to be put end-to-end for each treatment, where the
406 Z_{max} was assumed to be constant within the period of each simulation. Z_{max} values
407 were fixed to 30, 45, 75, 105 and 120 cm. The corresponding periods of the growth
408 cycle were given by Pilote which simulates the increase of Z_{max} as a function of the
409 cumulative degree-day temperatures. This temporal delimitation increased the
410 number of the simulations to total 1980 (11 treatments * 6 β * 6 ω_c * 5 end-to-end
411 sequences). However, through all the simulated period, drainage was calculated at the
412 depth of 120 cm, beyond which root density is assumed to become negligible.

413 Finally, for each of the simulations, the initial conditions were either predefined by
414 observed θ profiles during the first growth period with Z_{max} equal to 30 cm, or read
415 from the final time step of the previous simulation. On a personal computer (2.40 GHz
416 processor, 32-bits, 4.00 GB RAM), the run of all simulations took approximately 24
417 hours.

418

419 *Figure 6: Flowchart of the simulations conducted using Hydrus (2D/3D).*

420 **2.4. Statistical analysis of the results**

421 For each treatment, observed and simulated θ profiles (θ_{obs} and θ_{sim} , respectively)
422 were compared in order to determine the optimum simulation configuration (the
423 choice of β profile and ω_c levels). The statistics adopted for the comparison were the

424 correlation coefficient of Pearson (ρ) and the root-mean-square error (RMSE). In this
425 context, the errors were only different from zero when θ_{sim} fell outside the associated
426 confidence intervals (CI) of the measurements of θ_{obs} determined by the instrument
427 and calibration curves.

428 Both ρ and RMSE are complementary measures. The Pearson's ρ describes the
429 linear relationship between two continuous random variables regardless of their
430 values. Therefore, a high value of ρ means that a strong correlation between θ_{obs} and
431 θ_{sim} exists, indicating thus that water distribution pattern is reasonably simulated
432 (parallel θ profiles). However, this does not mean that both simulated and observed
433 profiles are close, hence the need for an estimate of the error by means of RMSE. To
434 determine whether the obtained RMSE values differed significantly following values of
435 β and ω_c statistical tests have to be performed. In this respect, as it was found that
436 errors $\{\varepsilon\} = \{|\theta_{obs} - \theta_{sim} - CI|\}$ increased with depth, their statistical distribution was
437 biased and did not adhere to normality. Therefore, the statistical analyses of RMSE
438 results was performed using nonparametric tests. Firstly, the Kruskal-Wallis (K-W) test
439 was used to determine whether β had a significant effect on ε for each ω_c value.
440 Secondly, when the results of the K-W test indicated a significant effect of β , the post-
441 hoc test of Dwass-Steel-Critchlow-Fligner pair-wise test was performed to determine
442 the significance of differences among the results.

4433. Results

444 3.1. Transpiration

445 The results of the simulated transpiration fluxes are illustrated in Figure [1](#) for
446 selected treatments of each watering method. In order to increase the readability of
447 the results, the cumulative transpiration curves ($T_{a\ cum}$) are illustrated only for the non
448 compensatory ($\omega_c = 1.0$) and the maximum compensatory ($\omega_c = 0.5$) RWU levels. The
449 corresponding differences in $T_{a\ cum}$ [mm] between those two latter cases are
450 summarized in Table [2](#).

451

452 *Figure 7: The cumulative transpiration curves $T_{a\ cum}$ simulated with non compensatory (left*
453 *column) and the maximum compensatory (right column) RWU levels.*

454 *Table 2: The differences between the maximum and the minimum simulated cumulative*
455 *transpiration $T_{a\ cum}$ for each treatment, using all β profiles (columns 2 to 5) and only those of*
456 *the “realistic” group (columns 6 to 9).*

457

458 **Surface-watering simulations**

459 In sprinkler treatments, using contrasted β profiles resulted in differences in $T_{a\ cum}$
460 within the range of 22 to 63 mm, representing respectively 4.5% and 14.0% (1-
461 min/max %) as shown in Table 2 (columns 2 and 3). These differences were higher for
462 fully-irrigated treatments than for those deficit-irrigated. However, for all irrigation
463 levels, the simulation with the maximum compensatory RWU level considerably
464 reduced the effect of β , to produce, in the cases of AspETM (12) and Asp70ETM (08),
465 almost identical total $T_{a\ cum}$ values (Table 2, columns 4 and 5).

466 Similar results were obtained for rainfed treatments, even though the simulated
467 $T_{a\ cum}$ showed a higher sensitivity to β . Contrasted β resulted in higher differences in
468 $T_{a\ cum}$, ranging from 28 to 87 mm which represent respectively 15.4% and 34.1%
469 (Table 2, columns 2 and 3). These differences were considerably reduced to about 13%
470 for all treatments when the compensatory RWU was activated (Table 2, columns 4 and
471 5).

472 The aforementioned differences in $T_{a\ cum}$ come principally from β_{Cst} and β_{Inv} . When
473 the latter are not considered, the simulated differences in $T_{a\ cum}$ become considerably
474 lower (Table 2, columns 6 to 9). The profiles β_{Asp} , β_{Obs} , β_{SDI-1} and β_{SDI-2} resulted in very
475 similar transpiration rates even when no compensatory RWU was considered. The
476 corresponding differences between $T_{a\ cum}$ maxima and minima were then between 2.0
477 and 7.5%, but in absolute water depth terms were all smaller than 16 mm.

478 The results of surface-watering simulations are not very sensitive to the spatial
479 distribution of root density RDD, provided that the latter decreases linearly or
480 exponentially with depth as observed for most realistic plant biomes by [Schenk and](#)
481 [Jackson \(2002\)](#). In this case, considering compensatory RWU yielded only a limited
482 effect on the simulated $T_{a\ cum}$, where the differences between $T_{a\ cum}$ minima and
483 maxima were all reduced by less than 13 mm (Table [2](#), columns 8 and 9), except for
484 the case of RF (11) where those differences were increased using the compensatory
485 uptake function.

486

487 **SDI simulations**

488 Root density distribution played a greater role in the determination of
489 transpiration rates in SDI treatments.

490 Considering for instance only β profiles of the “realistic” group (β_{Asp} , β_{Obs} , β_{SDI-1} ,
491 β_{SDI-2}): β_{Asp} and β_{SDI-1} systematically resulted in the lowest and the highest transpiration
492 rates, respectively (SDI results in Figure [7](#), left column). For non compensatory water
493 uptake, the differences between $T_{a\ cum}$ maxima and minima ranged from 37 mm (9.2%)
494 for the case of SDI (11) to as much as 83 mm (21.1%) for that of SDI (12), (Table [2](#),
495 columns 2 and 3). This greater difference obtained in 2012 was due to the higher
496 plant-dripline distance (65 cm) compared to 2008 and 2011 (40 and 30 cm,
497 respectively). Consequently, β profiles with maximum root densities located beneath
498 the plant row resulted in considerably lower water uptake compared to β_{SDI-1} .

499 However, activating the compensatory RWU function considerably reduced the
500 differences between $T_{a\ cum}$ maxima and minima, but this decrease strongly depended
501 on the plant-dripline distance. While those differences were reduced by 27 mm in both
502 2008 and 2011 (62% and 72%, respectively), the compensatory uptake resulted in a
503 limited reduction of only 12 mm (15%) in $T_{a\ cum}$ (max-min) in the case of 2012 (Table [2](#),
504 column 6 compared to column 8). Furthermore, for the case of 2012, more enhanced

505transpiration was simulated with β_{Obs} profile than with that of $\beta_{\text{SDI-2}}$ since the latter had
506less root density in the vicinity of the dripper compared to β_{Asp} .

507 **3.2. Drainage**

508 Similar to the previous section, the simulated drainage outfluxes below the root
509zone ($Z = 120$ cm) are illustrated only for a selected number of treatments (Figure 8).
510The differences in the cumulative drainage outfluxes ($\text{Drain}_{\text{cum}}$) are summarized in
511Table 3.

512

513 *Figure 8: Cumulative drainage/capillary rise outfluxes simulated with non compensatory (left*
514 *column) and the maximum compensatory (right column) RWU levels. Vertical bars represent*
515 *rainfall and irrigation events.*

516 *Table 3: The differences between the maximum and the minimum simulated cumulative*
517 *drainage $\text{Drain}_{\text{cum}}$ outfluxes for each treatments, using all β profiles (columns 2 and 3) and only*
518 *those of the “realistic” group (columns 4 and 5).*

519 Globally, the cumulative drainage outfluxes or capillary rise influxes followed the
520vertical distribution of root density, i.e. root profiles with higher root densities in lower
521soil layers resulted in systematically lower drainage rates or higher capillary rise
522(Figure 8). The simulations using β_{Inv} resulted in systematically the highest capillary
523rise rates, followed by the simulations issued from the β_{Cst} , then those of $\beta_{\text{SDI-1}}$ and $\beta_{\text{SDI-2}}$
524(both being quasi-identical for all sprinkler and rainfed simulations), then β_{Obs} and β_{Asp}
525last.

526

527**Surface-watering simulations**

528 Two groups of $\text{Drain}_{\text{cum}}$ curves are clearly distinguished in Figure 8: those resulting
529from the “realistic” (β_{Asp} , β_{Obs} , $\beta_{\text{SDI-1}}$ and $\beta_{\text{SDI-2}}$) and those from the “atypical” (β_{Cst} and
530 β_{Inv}) profiles.

531 The compensatory uptake had a limited effect on $\text{Drain}_{\text{cum}}$ (Table 3): it reduced
532 $\text{Drain}_{\text{cum}}$ by less than 6 mm in all simulations of the surface-watering treatments, but
533 failed to reduce differences of $\text{Drain}_{\text{cum}}$ (max-min). The latter were merely the same
534 with and without compensatory uptake. These results indicate that, in the case of
535 surface-watering conditions, the effect of the compensatory RWU function on the
536 reduction of the sensitivity of the simulated drainage is negligible.

537

538 **SDI simulations**

539 The sensitivity of drainage prediction to the spatial distribution of root density
540 was considerably higher under SDI conditions, as may be seen from Figure 8.

541 In addition to the vertical distribution of root density, the simulated $\text{Drain}_{\text{cum}}$
542 depended on the position of the plant row relative to the dripline. For instance, for
543 similar total irrigation depths in 2008, 2011 and 2012, the lowest drainage rates were
544 obtained with $\beta_{\text{SDI-1}}$ and $\beta_{\text{SDI-2}}$, in 2008 and 2011, but not in 2012 when $\beta_{\text{SDI-2}}$ resulted in
545 considerably higher drainage outfluxes due to higher plant-dripline distance.

546 Compensatory RWU efficiently reduced both the absolute value of drainage
547 outfluxes and the relative differences resulting from the contrasted β profiles (Table 3
548 columns 3 and 5 compared to columns 2 and 4, respectively). The plant-dripline
549 distance also conditioned the efficiency of the compensatory uptake function. The
550 reduction rates were greater with smaller plant-dripline distance : the simulated
551 $\text{Drain}_{\text{cum}}$ in the case of SDI (12), using β_{ASP} , was reduced by 35 mm for a ω_c of 0.5, while
552 only a reduction of 5.3 mm was obtained in the case of SDI (11), for the same
553 conditions (Table 3).

554 The compensatory uptake has thus a non negligible effect on the reduction of the
555 sensitivity of Hydrus (2D/3D) model to the β function, when it comes to drainage
556 simulation in SDI treatments. However, strong discrepancies in simulated drainage
557 outfluxes were still mainly explained by the β function. One may thus suggest that, in
558 the context of a macroscopic, empirical, RWU model as such implemented in Hydrus

559(2D/3D), reasonable predictions of drainage outfluxes may require the use of β profiles
560that are watering method-specific (water-tracking). This hypothesis is verified by the
561comparison of the observed θ profiles to those simulated, describing the RWU
562patterns.

563 **3.3. RWU patterns**

564 The values of Pearson correlation coefficient (ρ) between θ_{obs} and θ_{sim} for all
565scenarios are shown in Figure 9.

566

567 *Figure 9: Correlation coefficient of Pearson (ρ) between θ_{obs} and θ_{sim} profiles for all scenarios.*

568 *Only the positive ρ values are shown.*

569 Three main points are drawn from the results of the correlation test:

5701. The compensatory RWU process does not have a systematic effect on the
571 improvement of the predictions of RWU patterns: only the cases of AspETM (11)
572 and SDI (08) showed an increased value of ρ following an increase of ω_c , while for
573 the rest of the simulations the compensatory RWU had a very limited effect on ρ .

5742. For the β_{Cst} and β_{Inv} profiles, the poor values of ρ were improved with
575 compensatory RWU, but never reached those of the other realistic profiles (β_{Asp} ,
576 β_{Obs} , β_{SDI-1} and β_{SDI-2}). This shows the limits of the efficiency of the compensatory
577 RWU when used with a poor representation of root density.

5783. Water-tracking β profiles result in the best correlations, with and without
579 compensatory uptake: highest ρ values were obtained with β_{Asp} and β_{SDI-1}
580 respectively in surface-watering and SDI simulations.

581 The effects of ω_c on ρ for each β are further examined via the RMSE values,
582summarized in Table 4 for the simulations of the non compensatory (a) and the
583compensatory (b) water uptake level of 0.5.

584

585 *Table 4: Root-mean-squared errors (RMSE) [-] between θ_{sim} and θ_{obs} profiles for non*
586 *compensatory (a) and compensatory uptake (b) simulations. RMSE values followed by the*
587 *same letters indicate no statistically significant differences ($\alpha = 0.5$).*

588

589 The results of the ρ statistic are confirmed by RMSE values: poor predictions of θ
590 using β_{Cst} and β_{Inv} but better predictions using the β profiles of the “realistic” group.
591 Moreover, all “realistic” profiles yielded simulations with similar RMSE values, while
592 those of β_{Cst} and β_{Inv} resulted in significantly ($\alpha = 0.5$) higher RMSE in most
593 simulations. The lowest errors were obtained with β_{Asp} for most surface-watering
594 treatments, while the lowest errors in SDI treatments were obtained with the β_{SDI-1}
595 profile.

596 While the differences in RMSE among simulations were reduced with
597 compensatory RWU, their absolute values were unexpectedly increased for most
598 simulations (Table 4b compared to Table 4a). To explain this increase, it will be
599 necessary to graphically compare θ_{sim} to θ_{obs} profiles for both compensatory and non
600 compensatory RWU simulations. This comparison is only performed for selected cases.
601 The reader may refer to the supplementary materials to get access to the integrity of
602 simulation results.

603

604 **Surface-watering simulations**

605 *Figure 10: Comparison between θ_{sim} and θ_{obs} for all rainfed treatments, for non and maximum*
606 *compensatory RWU level. The horizontal bars represent measurement errors corresponding to*
607 *the neutron probe calibration equation.*

608 Reasonable agreements between θ_{sim} and θ_{obs} were obtained without
609 compensatory RWU in rainfed treatments (Figure 10, rows 1, 3 and 5). Using the
610 “realistic” β profiles resulted in predictions of θ within the observation confidence

611 intervals in RF (08) and RF (11), but slightly overestimated θ in deep soil layers in RF
612 (12). In contrast, using β_{Cst} and β_{Inv} resulted in significantly higher and lower θ values
613 in upper and lower soil layers, respectively.

614 The simulation with compensatory RWU slightly improved the predictions of θ in
615 RF (11) and RF (12), by an enhanced water uptake in deeper soil layers ($Z \geq 40$ cm),
616 (Figure 10, rows 4 and 6). However, it led to an insignificant reduction of the predicted
617 θ values (the θ profile remained within the confidence interval of measurements) when
618 the β_{Asp} was used in the case of RF (08), (Figure 10, row 2). This implies that the
619 resulting increase of 59 mm (35%) in $T_{a\ cum}$ obtained with the compensatory uptake
620 using β_{Asp} in 2008 is insignificant, and may thus be associated to the sensitivity of
621 Hydrus (2D/3D) to the spatial distribution of root density. Moreover, in RF (08) the
622 compensatory RWU led to significantly underestimate θ in deep soil layer, when β_{Asp}
623 was not used. This indicates that root density distribution is the factor that mostly
624 determine water uptake pattern, with and without the compensatory uptake function.
625 Furthermore, these results suggest that a compensatory mechanism did not take place
626 in the rainfed treatment of 2008, and that for rainfed treatments of 2011 and 2012,
627 improvements in water-content predictions may have simply been achieved by
628 modifying the parameters of the Feddes stress function (more tolerance to drought).

629 Similar results were obtained concerning the deficit-irrigated sprinkler treatments
630 (data not shown), but with the compensatory function slightly improving predictions of
631 θ in upper soil layers by an enhanced water uptake following watering. Nonetheless,
632 this enhanced uptake activity failed to mimic water uptake pattern in the more
633 dynamic watering conditions of the fully irrigated sprinkler treatments (AspETM 11 and
634 AspETM 12), as shown in Figure 11.

635
636 *Figure 11: Comparison between θ_{sim} and θ_{obs} for the fully-irrigated sprinkler treatments, for non*
637 *and maximum compensatory RWU level. The horizontal bars represent measurement errors*
638 *corresponding to the neutron probe calibration equation.*

639 Strong discrepancies were obtained in the fully-irrigated sprinkler treatments
640 between all θ_{sim} and θ_{obs} (Figure 11). From mid-season (DOY 170-180), all simulated
641 profiles showed a systematic overestimation of RWU in soil layers between 40 and 90
642 cm depths, and underestimated RWU in shallow soil layers. Given the reasonable
643 estimations of plant water requirements by Pilote (Appendix A1) and the fact that
644 irrigation and rainfall amounts were gauged directly in the vicinity of the instrumented
645 plots; it is unlikely that those discrepancies come from errors in the estimations in
646 either of T_a or water influxes rates.

647 When these discrepancies are further prone to increase with compensatory RWU
648 (see values of RMSE in Table 4b compared to Table 4a), one may then suggest that
649 such systematic discrepancies may only be suppressed by changing the root profile,
650 by increasing root density in the upper layers. This hypothesis was verified by
651 performing the simulations of both fully-irrigated treatments using a new root profile:
652 β_{ETM} . The root density of β_{ETM} is horizontally constant, but the density index
653 (adimensional) decreases linearly from 1.0 to 0.1 between depths of 0.0 and 30.0 cm,
654 then decreases linearly to reach 0.0 at a depth of 120.0 cm. These simulations were
655 only performed for two compensation levels : $\omega_c = 1.0$ and $\omega_c = 0.5$. The resulting θ
656 profiles are shown in Figure 12 only for simulations using β_{ASP} and β_{ETM} .

657
658 *Figure 12: Comparison between θ_{sim} and θ_{obs} for the fully-irrigated treatments. The simulations*
659 *were conducted using β_{ASP} and β_{ETM} profiles, for non and maximum compensatory RWU level.*
660 *The horizontal bars represent measurement errors corresponding to the neutron probe*
661 *calibration equation.*

662 Substantial improvements were obtained when β_{ETM} profile was used (Figure 12).
663 Better agreements between θ_{sim} and θ_{obs} were achieved for both ω_c values in AspETM
664 (12), but only for $\omega_c = 1.0$ (non compensatory uptake) in the case of AspETM (11). In
665 the latter case, $T_{a\ cum}$ was equal to 459 mm compared to 502 mm with compensatory

666uptake, i.e. an overestimation of 43 mm (9.4%) resulted from considering
667compensatory RWU.

668 This result confirms the former observations, in rainfed and deficit-irrigated
669sprinkler treatments, on the role of the β function being the main factor to determine
670water extraction pattern. In addition, this result points out to the possibility of an
671overestimation of transpiration when the compensatory uptake is considered.

672

673SDI simulations

674 Due to the inherent high spatial heterogeneity of soil water-content in SDI
675treatments, the comparison between θ_{sim} and θ_{obs} was performed on two verticals: the
676first on the crop row and the second in the immediate vicinity of the dripline
677(Figure 13) where measures of θ were only available in 2011 and 2012.

678

679 *Figure 13: Comparison between θ_{sim} and θ_{obs} under plant row and dripline for SDI (11) and SDI*
680 *(12), for non and maximum compensatory RWU levels. The horizontal bars represent*
681 *measurement errors corresponding to the neutron probe calibration equation.*

682 Both β and the compensatory RWU function were determinant factors to achieve
683reasonable predictions of θ profiles. Best agreements between θ_{obs} and θ_{sim} were
684obtained under both crop row and dripline when β_{SDI-1} was used in combination with
685the maximum compensatory RWU level (Figures 13). An interesting observation in
686Figure 13 is that of SDI (12) on DOY 214 and 242, where β_{SDI-1} allowed to obtain
687remarkably close predictions of θ profile, despite the relatively long plant-dripline
688distance of 65 cm. However, in some cases the compensatory RWU resulted in
689significant underestimation of θ_{sim} in upper soil layers under the crop row during earlier
690growth stages .

691 The results indicate that RWU is strongly underestimated if the compensatory
692RWU is not considered. Moreover, even for the maximum compensatory level, RWU is
693underestimated if β_{SDI-1} is not used (e.g., final observation dates in Figure 13). For

694instance, for SDI (08), SDI (11) and SDI (12), using β_{ASP} instead of β_{SDI-1} underestimate
695plant transpiration by respectively 43, 37 and 83 mm with non compensatory RWU, or
696respectively by 16, 10 and 71 mm when a compensatory RWU is considered.

697 Due to the more dynamic pattern of water allocation in SDI treatments (by both
698rainfall and dripline), maximum root activity is expected to alternate between the soil
699regions at surface and near the dripper, an activity that a static root density profile fail
700to mimic. Using the compensatory RWU allowed to overcome this shortcoming of static
701 β profiles. However, reasonable predictions of RWU activity was only achieved
702combining a high compensatory RWU level with a water-tracking root density profile.
703The latter was then found to be the determinant factor for reasonable RWU simulation
704in SDI treatments.

7054. Discussion

706 4.1. The efficiency of the compensatory root water uptake function ϕ

707 Let us recall the definition of the compensatory RWU process as proposed in the
708pioneer work of [Jarvis \(1989\)](#): the ability of plants to compensate stress-induced
709reduction of water uptake in one part of the root zone by an enhanced uptake from
710other parts where soil water is more readily available. On the one hand, we showed
711that using the compensatory RWU function efficiently increased the values of ρ
712between observed and simulated θ profiles, indicating thus better “overall” mimicking
713of RWU pattern. However, on the other hand, the compensatory RWU led to larger
714prediction errors $\{|\theta_{obs} - \theta_{sim} - CI|\}$, which means that these errors came from enhanced
715water uptake in the “wrong” soil regions:

7161. In surface-watering simulations, the enhanced RWU by the compensatory
717 process took place mainly in deep soil layers. When rainfed treatments are
718 considered, RWU was not observed to be enhanced in deep soil layers in all
719 treatments. When fully-irrigated sprinkler treatments are considered, enhanced

720 RWU was observed in the uppermost soil layers due to the surface irrigation
721 regime.

722. In subsurface drip irrigation simulations, the enhanced RWU by the
723 compensatory process led to obtain remarkably good agreements between θ_{obs} and
724 θ_{sim} under the dripline when root density was adequately described. However, since
725 the compensatory rate is proportional to the T_a/T_p ratio (Eq. 5) rather than soil-
726 water content spatial distribution, the enhanced RWU was not limited to soil
727 regions around the drip water source, but occurred in the entire root zone.
728 Consequently, simulated enhanced RWU also occurred beneath the plant row
729 contrarily to observations.

730 Points 1 and 2 indicate that the compensatory RWU process may hardly be seen
731 as a response to the total plant stress status ratio T_a/T_p . Our results suggest that the
732 compensatory RWU pattern depends on the distribution of water through the soil
733 domain, rather than plant water deficit.

734 The results of this study are in agreement with a recent study on RWU pattern
735 conducted by [Javaux et al. \(2013\)](#). Using a physically-based macroscopic RWU model
736 developed by [Couvreur et al. \(2012\)](#), [Javaux et al. \(2013\)](#) found that the compensatory
737 RWU rate is independent from the ratio (ω/ω_c) . Both studies of [Couvreur et al. \(2012\)](#)
738 and [Javaux et al. \(2013\)](#) further proposed a decoupling of the water stress function
739 $\gamma(h)$ from that of the compensatory RWU, since the latter occurred even at very low
740 water potential levels. The compensatory RWU is thus perceived as the redistribution
741 of RWU due to a nonuniform water head distribution at the soil-root interface.

742 A number of examples of empirical compensatory RWU functions which are
743 independent from the T_a/T_p ratio exists in literature (e.g., [Bouten et al., 1992](#); [Lai and](#)
744 [Katul., 2000](#); [Li et al., 2001](#)). However, such models are also shown to be highly
745 dependent on root density (see [Heinen, 2014](#) for the case of the function of [Bouten et](#)
746 [al., 1992](#)), and still couple the water stress and compensatory processes. An

747 interesting approach to RWU simulation would be to extrapolate the propositions of
748 [Couvreur et al. \(2012\)](#) and [Javaux et al. \(2013\)](#) for the modeling of empirical
749 macroscopic RWU models. Such extrapolation may replace Equation 4 for the
750 calculation of RWU by another one of the form:

$$751 \quad S = T_p \beta(x, z) [\gamma(h) + \phi(h)] \quad (8)$$

752 The quantity $T_p \beta(x, z) \gamma(h)$ in Equation 8 represents RWU in standard conditions
753 (uniform soil water potential over the entire root zone), while the quantity $T_p \beta(x, z) \phi$
754 (h) represents the instantaneous adjustment of RWU distribution to cope with the
755 variations of soil water potential in the root zone. For example, the distribution of the
756 values of $\phi(h)$ may be deduced from moment analysis of the spatial distribution of soil
757 water potential. Furthermore, analogously to the formula proposed by [Couvreur et al.](#)
758 [\(2012\)](#), the sign of $\phi(h)$ may be positive (enhanced uptake) or negative (hydraulic lift).
759 However, more research is needed to propose a formula for the $\phi(h)$ that respects the
760 condition ($T_a \leq T_p$). Such work is beyond the scope of the present study.

761 4.2. The role of root density distribution

762 [Warrick and Or \(2007\)](#) stated that “often no distinction is made between root
763 length density and root activity or uptake”. Maintaining the current formula of the RWU
764 function (Eq. 2 and 4) implies that all roots are considered active. Therefore, β must
765 reasonably reflect the RWU activity. Both by experimental (e.g. [Homaei et al., 2002](#);
766 [Hodge, 2004](#)) and numerical analysis ([Bruckler et al., 2004](#); [Faria et al., 2010](#)), RWU
767 activity was widely reported to employ only a limited percentage of the entire root
768 system.

769 It was shown in section 3 that β has a determinant role in the prediction of RWU
770 pattern, under all water stress conditions. It was shown in Figure 9 and Table 4 that
771 better predictions of θ were obtained when root profiles specific to the watering
772 method were used: β_{ETM} in fully-irrigated sprinkler treatments, β_{ASp} in deficit-irrigated
773 sprinkler treatments and β_{SDI-1} in SDI treatments.

774 By numerical analysis with a physically-based RWU model, [Bruckler et al. \(2004\)](#)
775 found that surface watering events resulted in roots having high instantaneous water
776 uptake rates. Consequently, only a limited number of roots assured the full water
777 requirements by plants. The results of the present study are in agreements with the
778 findings of [Bruckler et al. \(2004\)](#). It was shown in section [3](#) that a correct prediction of
779 RWU pattern, in fully-irrigated sprinkler treatments, was obtained if and only if a
780 specific β profile (β_{ETM}), having the maximum root density in the uppermost soil layers,
781 was used. In SDI treatments, reasonable prediction of RWU pattern required both a
782 high compensatory RWU level and a root profile with maximum density near the
783 dripper.

784 These results plead in favor of the use of water-tracking RWU, particularly in the
785 case of locally-watered soil domains where a reasonable prediction of RWU pattern
786 requires both a pertinent description of the spatial distribution of root density and a
787 high compensatory uptake level. In that sense, when Equation [4](#) is used to describe
788 RWU, the β function should not only reflect the potential RWU pattern according to
789 root density, but also according to the expected soil-water availability (i.e., watering
790 influx distribution). This recalls the early definitions of β as “root effectiveness
791 function” as stated by [Whisler et al. \(1968\)](#). Thus, by using a watering method-specific
792 β , the aim is to increase the probability of an enhanced water uptake in predefined
793 wetter soil regions.

794 Another issue related to root density distribution is its relation to the simulated
795 water outfluxes from the soil domain. T_a is the integral of the spatially-distributed RWU
796 (Eq. [7](#)). Therefore, it is expected that different root density profiles may lead to similar
797 transpiration rates. By comparing 4 different RWU models, going from empirical
798 macroscopic to physically-based microscopic, [de Willigen et al. \(2012\)](#) found that
799 differences in total transpiration were small compared to those of the simulated soil-
800 water dynamics. The authors explained their results by the feedback process between
801 the RWU and water flow models. This shows that the determination of the “best” RDD

802 function or compensatory RWU level based solely on comparisons to measured T_a is a
803 condition necessary but not sufficient. This confirms the pertinence of the choice to
804 base our analysis on the comparison between θ_{sim} and θ_{obs} , which not only allows an
805 insight to RWU pattern, but also assures mass balance conservation ($T_{a,cum}$).

806 Finally, our results showed that using a uniform β profile, when relevant
807 information on root system is missing, may lead to poor estimates of plant
808 transpiration and drainage fluxes as well as RWU pattern, under both surface and
809 subsurface waterings. Such consideration may thus bias the evaluation of optimum
810 SDI design when an inappropriate β profile is used, as performed by [Kandelous et al.](#)
811 (2012).

812 **4.3. The performance of the empirical macroscopic RWU approach**

813 The empirical macroscopic RWU models are often subject to critical comments
814 ranging from too little biophysical basis ([Skaggs et al., 2006](#); [Javaux et al., 2008](#);
815 [Schneider et al., 2010](#); [Javaux et al., 2013](#)) to too many parameters requiring
816 calibration ([Feddes et al., 2001](#); [Homaee et al., 2002](#); [Couvreur et al., 2012](#); [de](#)
817 [Willigen et al., 2012](#)), and questionable performance in heterogeneous soils ([Kuhlmann](#)
818 [et al., 2012](#)).

819 However, the results obtained in this study show a rather robust performance of
820 this RWU approach in stratified soil profiles, under contrasted watering methods,
821 watering dynamics and water stress status, provided that adequate descriptions of the
822 root density distribution and compensatory levels are used. These were nonetheless
823 the results of rather simple cases of a mono-crop cultivated soil domain, and are thus
824 subject to vary for more complex systems, where more sophisticated physically-based
825 models may be more efficient.

826 **5. Conclusions**

827 Using an empirical macroscopic root water uptake model integrated in a
828 physically-based soil water flow model, a numerical analysis was performed to

829 examine the sensitivity of simulated actual transpiration (T_a), drainage ($Drain_a$) and
830 root water uptake (RWU) patterns to both root density distribution (RDD) and
831 compensatory RWU functions. The numerical analysis was based on simulations of
832 water transfer in a vertical 2D soil domain cultivated with maize, irrigated by surface
833 (sprinkler) or subsurface (SDI) systems, or rainfed. The simulations were compared to
834 experimental data to estimate the errors in drainage rates due to uncertainties in the
835 RDD, to study the effect of the compensatory RWU function on the sensitivity to RDD,
836 and to verify whether the use of a water-tracking root density profile replaces the need
837 for compensatory RWU functions. The principal findings of this study may be
838 summarized in the following points:

8391. The simulation of T_a , showed to be of low sensitivity to RDD in sprinkler-irrigated
840 (Asp) and rainfed (RF) treatments, provided that root density decreases linearly or
841 exponentially with depth. In contrast, RDD played a greater role in the
842 determination of T_a in the case of subsurface drip-irrigated (SDI) treatments.

8432. The simulation of $Drain_a$ was found to vary considerably in all cases with the
844 RDD.

8453. The compensatory RWU function further reduced the sensitivity of the simulated
846 T_a to RDD in surface-watering treatments and, to a lesser extent, in SDI treatments.
847 The efficiency of the compensatory RWU function in SDI simulations depended on
848 the plant-dripline distance.

8494. The compensatory RWU function had low or no effect on the reduction of the
850 sensitivity of the simulated $Drain_a$ to RDD in surface-watering treatments. In
851 contrast, compensatory RWU function played a considerable role in the reduction of
852 differences resulting from different RDD profiles in SDI simulations. However,
853 reasonable predictions of the RWU pattern were only achieved when a RDD profile
854 specific to SDI was used with a high compensatory RWU level.

8555. Using an empirical macroscopic RWU function, it was shown that the main
856 condition for reasonable estimation of T_a , $Drain_a$ and RWU pattern was to use water-
857 tracking RWU.

8586. Finally, the results suggest that the use of the compensatory RWU function of
859 [Jarvis \(1989\)](#) is recommended for simulations with local water influx simulations
860 (SDI), but questionable performance is expected in simulations where water influx is
861 uniform over the soil domain surface (sprinkler).

862 **Acknowledgments**

863 The University of Aleppo, Syria, is greatly acknowledged for the PhD scholarship granted to Rami
864 ALBASHA. The authors gratefully acknowledge Mr. Christian LEDUC, Mr. François AFFHOLDER and Mme.
865 Séverine TOMAS for critically reading the manuscript. The authors also thank Mr. Jean-Marie LOPEZ, Mr.
866 Patrick ROSIQUE and Mr. Augustin LUXIN for their assistance in data collection.

867 **References**

- 868 Adiku, S. G. K., Rose, C. W., Braddock, R. D., Ozier-Lafontaine, H., 2000. On the simulation of
869 root water extraction: Examination of a minimum energy hypothesis. *Soil Science* 165 (3),
870 226 - 236.
- 871 Allen, R., Pereira, L., Raes, D., Smith, M., 1998. Crop evapotranspiration - guidelines for
872 computing crop water requirements. Paper 56, Food and Agricultural Organization of the
873 United Nations.
- 874 Allison, B., Fechter, J., Leucht, A., Sivakumar, M., 1993. The use of the Ceres-Millet model for
875 production strategy analysis in south west Niger. In: 15th Congress on Irrigation and
876 Drainage. 2nd Workshop on Crop Water Models. Session III. The Hague, the Netherlands., p.
877 17.
- 878 Baluska, F., Mancuso, S., Volkmann, D., Barlow, P. W., 2009. The 'root-brain' hypothesis of
879 Charles and Francis Darwin: Revival after more than 125 years. *Plant Signaling & Behavior* 4
880 (12), 1121 - 1127.
- 881 Beudez, N., Doussan, C., Lefeuvre-Mesgouez, G., Mesgouez, A., 2013. Influence of three root
882 spatial arrangement on soil water flow and uptake. Results from an explicit and an
883 equivalent, upscaled, model. *Procedia Environmental Sciences* 19, 37 - 46, Four Decades of
884 Progress in Monitoring and Modeling of Processes in the Soil-Plant- Atmosphere System:
885 Applications and Challenges.
- 886 Bouten, W., Heimovaara, T. J., Tiktak, A., 1992. Spatial patterns of throughfall and soil water
887 dynamics in a douglas fir stand. *Water Resources Research* 28 (12), 3227 - 3233.
- 888 Bruckler, L., Lafolie, F., Doussan, C., Bussièrès, F., 2004. Modeling soil-root water transport with
889 non-uniform water supply and heterogeneous root distribution. *Plant and Soil* 260, 205 - 224.
- 890 Couvreur, V., Vanderborght, J., Javaux, M., 2012. A simple three-dimensional macroscopic root
891 water uptake model based on the hydraulic architecture approach. *Hydrology and Earth
892 System Sciences* 16 (8), 2957 - 2971.
- 893 Coelho, E. F., Or, D., 1996. A Parametric Model for Two-Dimensional Water Uptake Intensity by
894 Corn Roots under Drip Irrigation. *Soil Science Society of America Journal* 60, 1039-1049.
- 895 Coelho, E. F., Or, D., 1999. Root distribution and water uptake patterns of corn under surface
896 and subsurface drip irrigation. *Plant and Soil* 206, 123 - 136.

- 897 Darwin, C. (assisted by Darwin, F.), 1880. *The Power of Movements in Plants*. John Murray,
898 London (<http://darwin-online.org.uk/>).
- 899 de Jong van Lier, Q., van Dam, J. C., Metselaar, K., de Jong, R., Duijnisveld, W. H. M., 2008.
900 Macroscopic root water uptake distribution using a matric flux potential approach. *Vadose*
901 *Zone Journal* 7 (3), 1065 - 1078.
- 902 de Willigen, P., van Dam, J. C., Javaux, M., Heinen, M., 2012. Root water uptake as simulated by
903 three soil water flow models. *Vadose Zone Journal* 11 (3), _.
- 904 Faria, L., Rocha, M., de Jong van Lier, Q., Casaroli, D., 2010. A split-pot experiment with
905 sorghum to test a root water uptake partitioning model. *Plant and Soil* 331 (1-2), 299 - 311.
- 906 Feddes, R., Kowalik, P., Zaradny, H., 1978. *Simulation of field water use and crop yield*.
907 *Simulation Monograph Series*. Pudoc, Wageningen, The Netherlands.
- 908 Feddes, R., Raats, P., 2004. *Unsaturated Zone Modelling: Progress, Challenges and Applications*.
909 Vol. 6 of Wageningen UR Frontis Series. Kluwer Academic, Dordrecht, The Netherlands, Ch.
910 *Parameterizing the soil-waterplant- root system*, pp. 95 - 141.
- 911 Feddes, R. A., Hoff, H., Bruen, M., Dawson, T., de Rosnay, P., Dirmeyer, P., Jackson, R. B., Kabat,
912 P., Kleidon, A., Lilly, A., Pitman, A. J., 2001. Modeling root water uptake in hydrological and
913 climate models. *Bulletin of the American Meteorological Society* 82 (12), 2797 - 2809.
- 914 Green, S. R., Clothier, B. E., 1995. Root water uptake by kiwifruit vines following partial wetting
915 of the root zone. *Plant and Soil* 173, 317 - 328.
- 916 Heinen, M., 2001. Fussim2: brief description of the simulation model and application to
917 fertigation scenarios. *Agronomie* 21 (4), 285 - 296.
- 918 Heinen, M., 2014. Compensation in root water uptake models combined with three-dimensional
919 root length density distribution. *Vadose Zone Journal* 13 (2), _.
- 920 Hodge, A., 2004. The plastic plant: root responses to heterogeneous supplies of nutrients. *New*
921 *Phytologist* 162 (1), 9 - 24.
- 922 Hodge, A., Berta, G., Doussan, C., Merchan, F., Crespi, M., 2009. Plant root growth, architecture
923 and function. *Plant and Soil* 321 (1-2), 153 - 187.
- 924 Homae, M., Feddes, R., Dirksen, C., 2002. Simulation of root water uptake: II. non-uniform
925 transient water stress using different reduction functions. *Agricultural Water Management* 57
926 (2), 111 - 126.

- 927 Hopmans, J. W., Bristow, K. L., 2002. Current capabilities and future needs of root water and
928 nutrient uptake modeling. Vol. 77 of *Advances in Agronomy*. Academic Press, pp. 103 - 183.
- 929 Jarvis, N., 1989. A simple empirical model of root water uptake. *Journal of Hydrology* 107 (1-4),
930 57 - 72.
- 931 Javaux, M., Couvreur, V., Vanderborght, J., Vereecken, H., 2013. Root water uptake: From three-
932 dimensional biophysical processes to macroscopic modeling approaches. *Vadose Zone*
933 *Journal* 12 (4), _.
- 934 Javaux, M., Schröder, T., Vanderborght, J., Vereecken, H., 2008. Use of a three-dimensional
935 detailed modeling approach for predicting root water uptake. *Vadose Zone Journal* 7 (3),
936 1079 - 1088.
- 937 Kandelous, M. M., Kamai, T., Vrugt, J. A., Simunek, J., Hanson, B., Hopmans, J. W., 2012.
938 Evaluation of subsurface drip irrigation design and management parameters for alfalfa.
939 *Agricultural Water Management* 109 (0), 81 - 93.
- 940 Khaledian, M., Mailhol, J., Ruelle, P., Rosique, P., 2009. Adapting pilote model for water and yield
941 management under direct seeding system: The case of corn and durum wheat in a
942 mediterranean context. *Agricultural Water Management* 96 (5), 757 - 770.
- 943 Kuhlmann, A., Neuweiler, I., van der Zee, S. E. A. T. M., Helmig, R., 2012. Influence of soil
944 structure and root water uptake strategy on unsaturated flow in heterogeneous media.
945 *Water Resources Research* 48 (2), _.
- 946 Kramer, P., Boyer, J., 1995. *Water Relations of Plants and Soils*, Academic Press, San Diego, CA.
- 947 Klepper, B., 1991. Crop root system response to irrigation. *Irrigation Science* 12 (3), 105 - 108.
- 948 Lafolie, F., Guennelon, R., van Genuchten, M., 1989. Analysis of water flow under trickle
949 irrigation: I. theory and numerical solution. *Soil Science Society of America Journal* 53 (5),
950 1310 - 1318.
- 951 Lai, C.-T., Katul, G., 2000. The dynamic role of root-water uptake in coupling potential to actual
952 transpiration. *Advances in Water Resources* 23 (4), 427 - 439.
- 953 Leib, B., Caspari, H., Redulla, C., Andrews, P., Jabro, J., 2006. Partial rootzone drying and deficit
954 irrigation of 'fuji' apples in a semi-arid climate. *Irrigation Science* 24, 85 - 99.
- 955 Li, K. Y., De Jong, R., Boisvert, J. B., 2001. An exponential root-water-uptake model with water
956 stress compensation. *Journal of Hydrology* 252 (1-4), 189 - 204.

- 957 Mailhol, J. C., Olufayo, A. A., Ruelle, P., 1997. Sorghum and sunflower evapotranspiration and
958 yield from simulated leaf area index. *Agricultural Water Management* 35 (1-2), 167 - 182.
- 959 Mailhol, J. C., Ruelle, P., Walser, S., N., S., Dejean, C., 2011. Analysis of aet and yield predictions
960 under surface and buried drip irrigation systems using the crop model pilote and Hydrus-2D.
961 *Agricultural Water Management* 98 (6), 1033 - 1044.
- 962 Molz, F. J., 1981. Models of water transport in the soil-plant system: a review. *Water Resources*
963 *Research* 17 (5), 1245 - 1260.
- 964 Mualem, Y., 1976. A new model for predicting the hydraulic conductivity of unsaturated porous
965 media. *Water Resources Research* 12 (3), 513 - 522.
- 966 Mubarak, I., Mailhol, J. C., Angulo-Jaramillo, R., Bouarfa, S., Ruelle, P., 2009a. Effect of temporal
967 variability in soil hydraulic properties on simulated water transfer under high-frequency drip
968 irrigation. *Agricultural Water Management* 96 (11), 1547 - 1559.
- 969 Mubarak, I., Mailhol, J. C., Angulo-Jaramillo, R., Ruelle, P., Boivin, P., Khaledian, M., 2009b.
970 Temporal variability in soil hydraulic properties under drip irrigation. *Geoderma* 150 (1-2),
971 158 - 165.
- 972 Novák, V., 1981. The structure of evapotranspiration (in slovak) I. and II. *Vodohosp* 29, 476 -
973 492 and 581 - 582.
- 974 Oki, T., Kanae, S., 2006. Global hydrological cycles and world water resources. *Science* 313
975 (5790), 1068 - 1072.
- 976 Oster, J., Letey, J., Vaughan, P., Wu, L., Qadir, M., 2012. Comparison of transient state models
977 that include salinity and matric stress effects on plant yield. *Agricultural Water Management*
978 103, 167 - 175.
- 979 Pang, X. P., Letey, J., 1998. Development and evaluation of enviro-gro, an integrated water,
980 salinity, and nitrogen model. *Soil Science Society of America Journal* 62 (5), 1418 - 1427.
- 981 Penman, H. L., 1948. Natural evaporation from open water, bare soil and grass. *Proceedings of*
982 *the Royal Society of London. Series A. Mathematical and Physical Sciences* 193 (1032), 120 -
983 145.
- 984 Raats, P., 2007. Uptake of water from soils by plant roots. *Transport in Porous Media* 68, 5 - 28.
- 985 Richards, L. A., 1931. Capillary conduction of liquids through porous mediums. *Physics* 1, 318 -
986 333.

- 987 Ritchie, J. T., 1972. Model for predicting evaporation from a row crop with incomplete cover.
988 *Water Resources Research* 8 (5), 1204 - 1213.
- 989 Schenk, H. J., Jackson, R. B., aug 2002. The global biogeography of roots. *Ecological*
990 *Monographs* 72 (3), 311 - 328.
- 991 Schneider, C. L., Attinger, S., Delfs, J.-O., Hildebrandt, A., 2010. Implementing small scale
992 processes at the soil-plant interface - the role of root architectures for calculating root water
993 uptake profiles. *Hydrology and Earth System Sciences* 14 (2), 279 - 289.
- 994 Shouse, P. J., Ayars, J. E., Simunek, J., 2011. Simulating root water uptake from a shallow saline
995 groundwater resource. *Agricultural Water Management* 98 (5), 784 - 790.
- 996 Simunek, J., Hopmans, J. W., 2009. Modeling compensated root water and nutrient uptake.
997 *Ecological Modelling* 220 (4), 505 - 521.
- 998 Simunek, J. J., van Genuchten, M. T., Sejna, M., 2008. Development and applications of the
999 *hydrus* and *stanmod* software packages and related codes. *Vadose Zone Journal* 7 (2), 587 -
1000 600.
- 1001 Skaggs, T. H., van Genuchten, M. T., Shouse, P. J., Poss, J. A., 2006. Macroscopic approaches to
1002 root water uptake as a function of water and salinity stress. *Agricultural Water Management*
1003 86 (1-2), 140 - 149.
- 1004 Subbaiah, R., 2011. A review of models for predicting soil water dynamics during trickle
1005 irrigation. *Irrigation Science* 31 (3), 225 - 258.
- 1006 Tardieu, F., Manichon, H., 1986. Caractérisation en tant que capteur d'eau de l'enracinement du
1007 maïs en parcelle cultivée. ii. - une méthode d'étude de la répartition verticale et horizontale
1008 des racines. *Agronomie* 6 (5), 415 - 425.
- 1009 van den Honert, T. H., 1948. Water transport in plants as a catenary process. *Discussions of the*
1010 *Faraday Society* 3, 146 - 153.
- 1011 van Genuchten, M. T., 1980. A closed-form equation for predicting the hydraulic conductivity of
1012 unsaturated soils. *Soil Science Society of America Journal* 44, 892 - 898.
- 1013 van Genuchten, M. T., 1987. A numerical model for water and solute movement in and below
1014 the root zone. Tech. Rep. 121, U.S. Salinity laboratory, USDA, ARS, Riverside, California.
- 1015 van Wijk, M. T., Bouten, W., 2001. Towards understanding tree root profiles: simulating
1016 hydrologically optimal strategies for root distribution. *Hydrology and Earth System Sciences*
1017 5 (4), 629 - 644.

1018Vrugt, J. A., van Wijk, M. T., Hopmans, J. W., Simunek, J., 2001. One-, two-, and three-
1019 dimensional root water uptake functions for transient modeling. *Water Resources Research*
1020 37 (10), 2457 - 2470.

1021Warrick, A. W., Or, D., 2007. 2. Soil water concepts. In: Freddie R. Lamm, J. E. A., Nakayama, F.
1022 S. (Eds.), *Microirrigation for Crop Production Design, Operation, and Management*. Vol. 13 of
1023 *Developments in Agricultural Engineering*. Elsevier, pp. 27 - 59.

1024Whisler, F. D., Klute, A., Millington, R. J., 1968. Analysis of steady-state evapotranspiration from
1025 a soil column. *Soil Science Society of America Journal* 32 (2), 167 - 174.

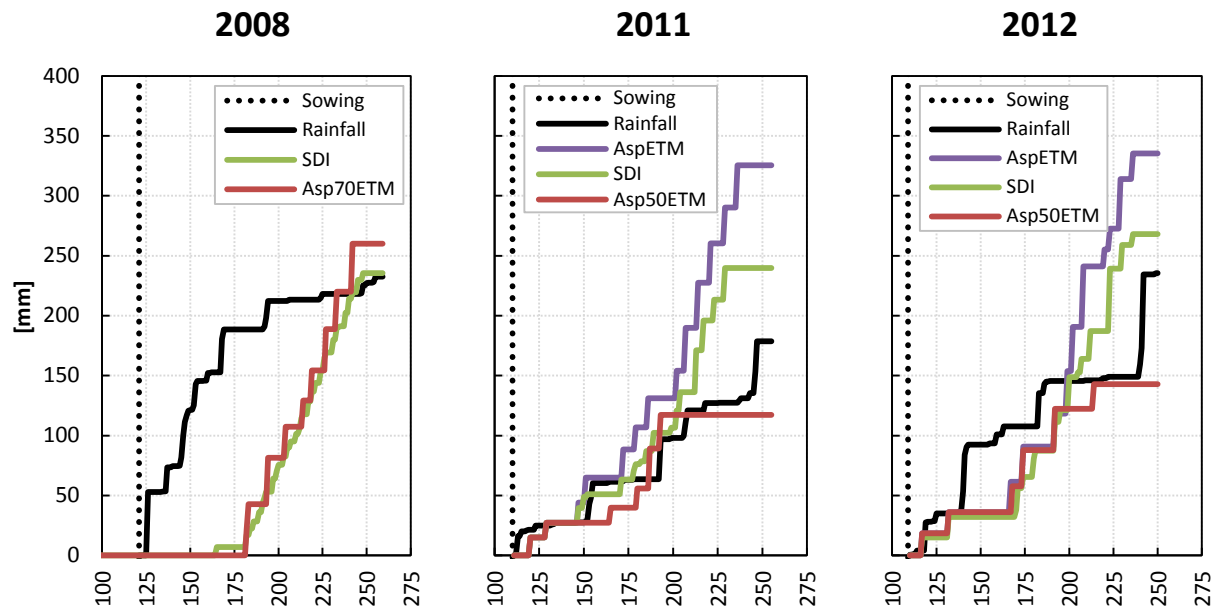


FIGURE 1 : Cumulative rainfall and irrigation quantities applied to all plots during the growing seasons 2008, 2011 and 2012.

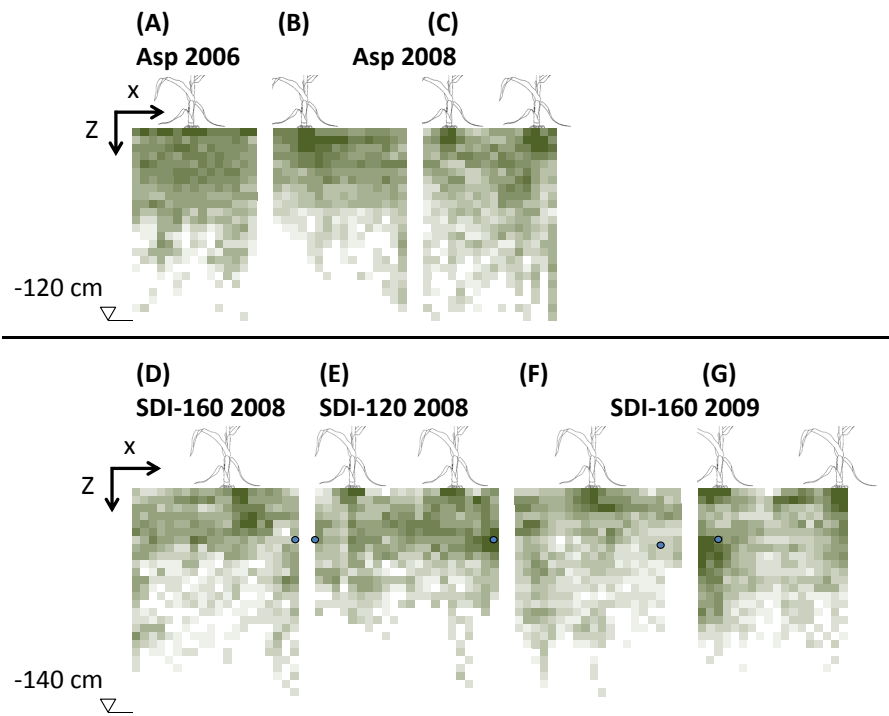


Figure 2: Observed root density profiles of Asp (A, B, C) and SDI (D, E, F, G) maize plots. Root density was evaluated visually following the method of Tardieu and Manchion (1986). The observed profiles come from different experimental campaigns as denoted for each profile.

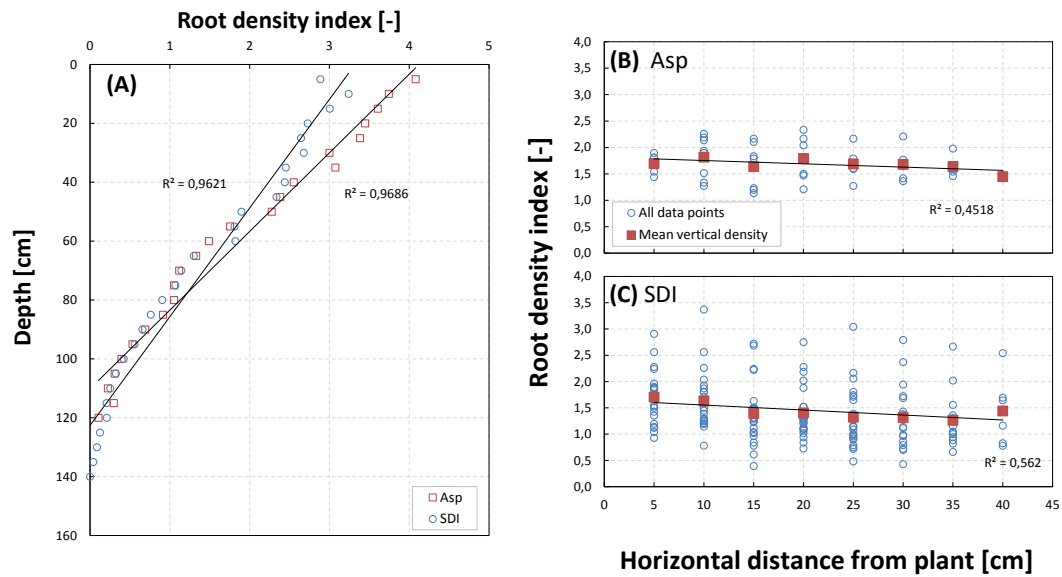


Figure 3: The mean horizontal root density distribution (A) for both Asp and SDI maize plots, and the mean vertical root density of Asp (B) and SDI (C).

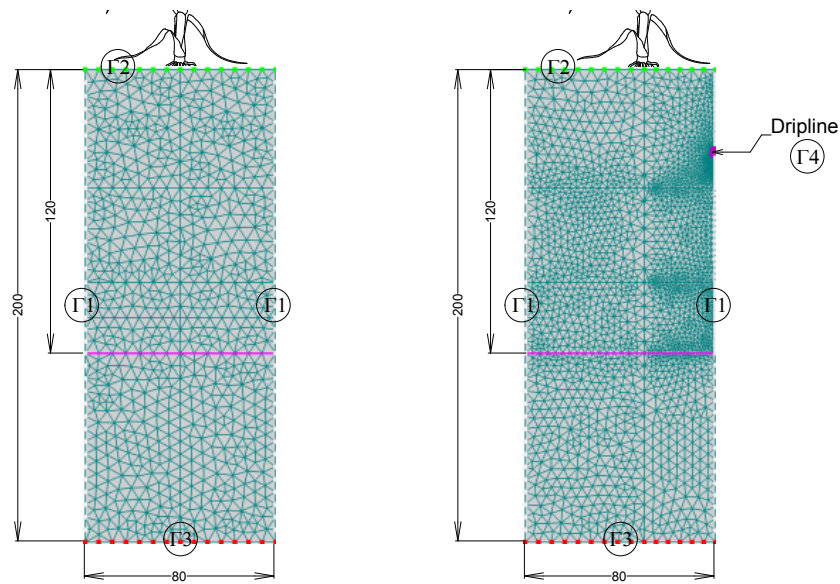


Figure 4: The geometry and boundary conditions (BC's) imposed to the soil domains with dimensions given in cm. Γ_1 is a zero horizontal flux BC, Γ_2 is an atmospheric BC, Γ_3 is a constant water-content BC and Γ_4 is a variable flux BC. The horizontal pink line at 120 cm represents the maximum root depth at which drainage was calculated.

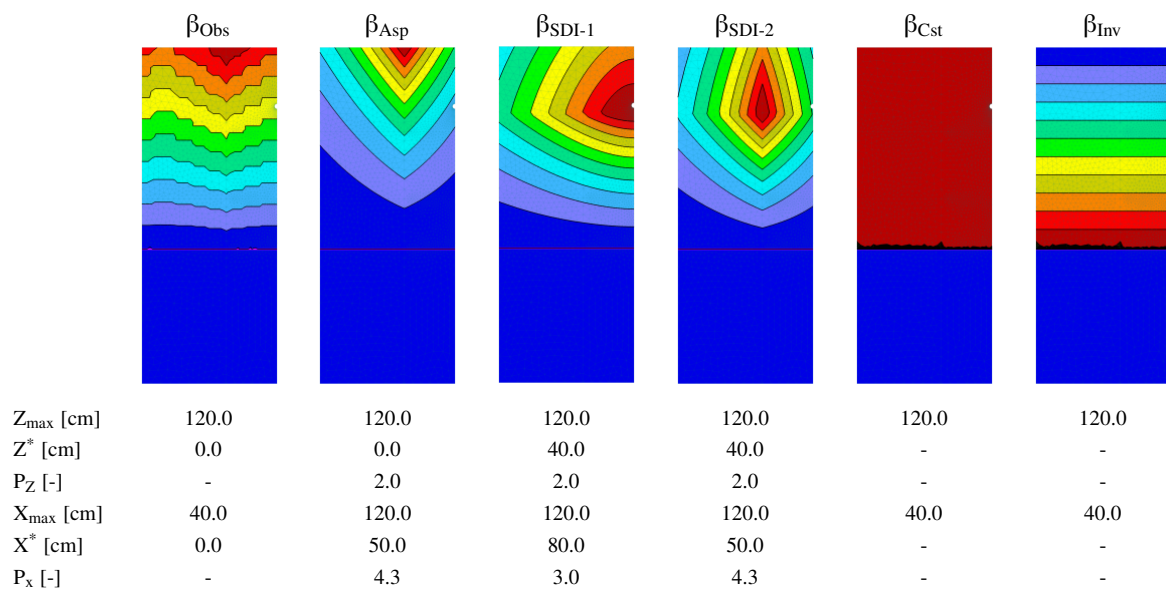


Figure 5: Root density profiles of fully-developed maize irrigated with SDI with driplines located on the right-side boundary at a depth of 40 cm. X^* and Z^* are the horizontal and vertical coordinates at which the root density is maximum. X_{\max} and Z_{\max} delimit the soil region occupied by roots. P_x and P_z are empirical shape parameters (specific to the function of ?).

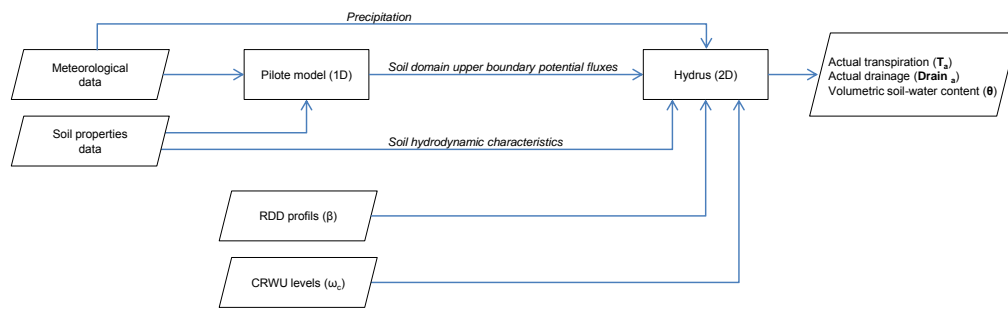


Figure 6: Flowchart of the simulations with Hydrus (2D/3D).

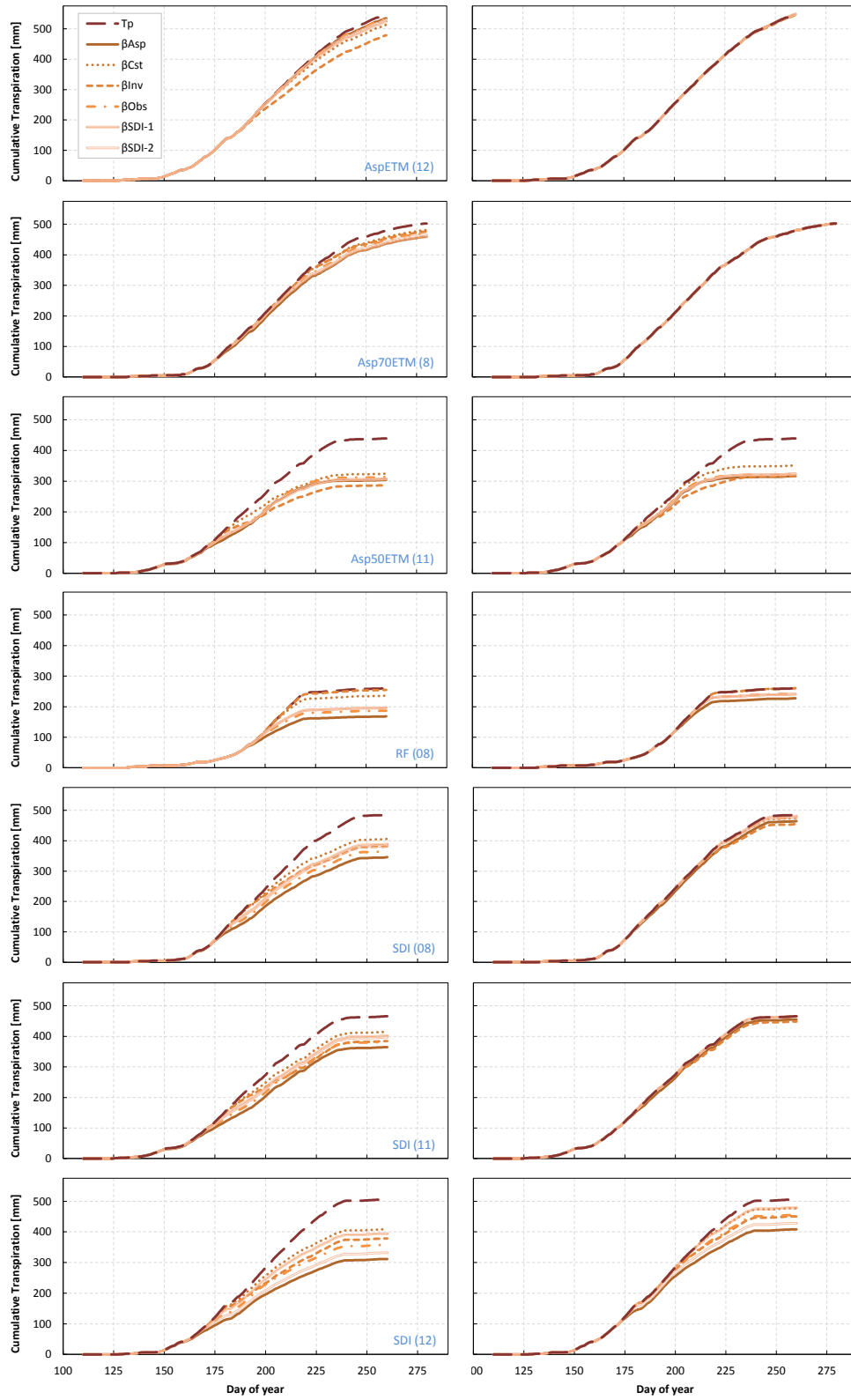


Figure 7: The cumulative transpiration curves $T_{a\ cum}$ simulated with non compensatory (left column) and the maximum compensatory (right column) RWU levels.

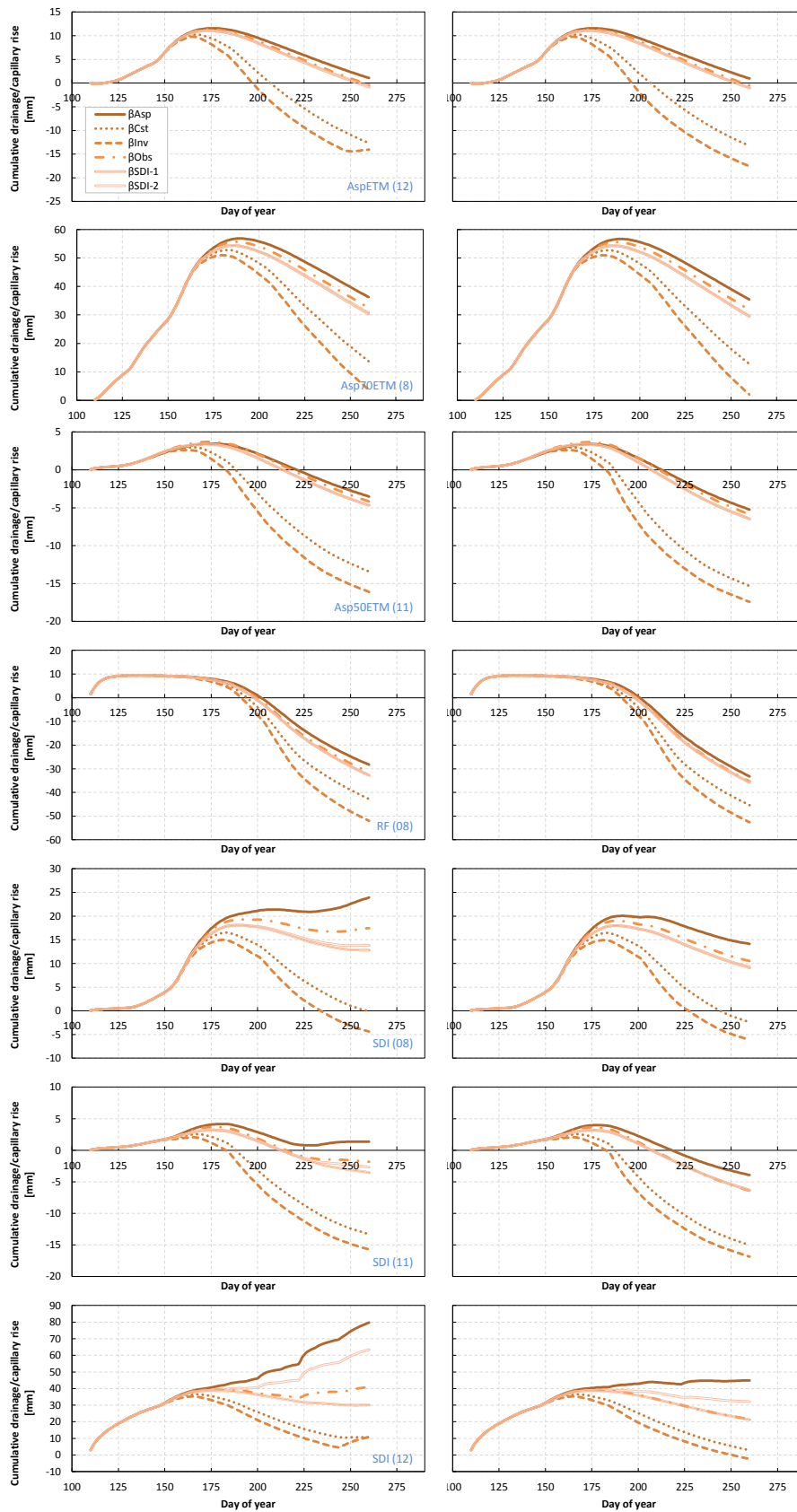


Figure 8: Cumulative drainage/capillary rise outfluxes simulated with non compensatory (left column) and the maximum compensatory (right column) RWU levels. Vertical bars represent rainfall and irrigation events.

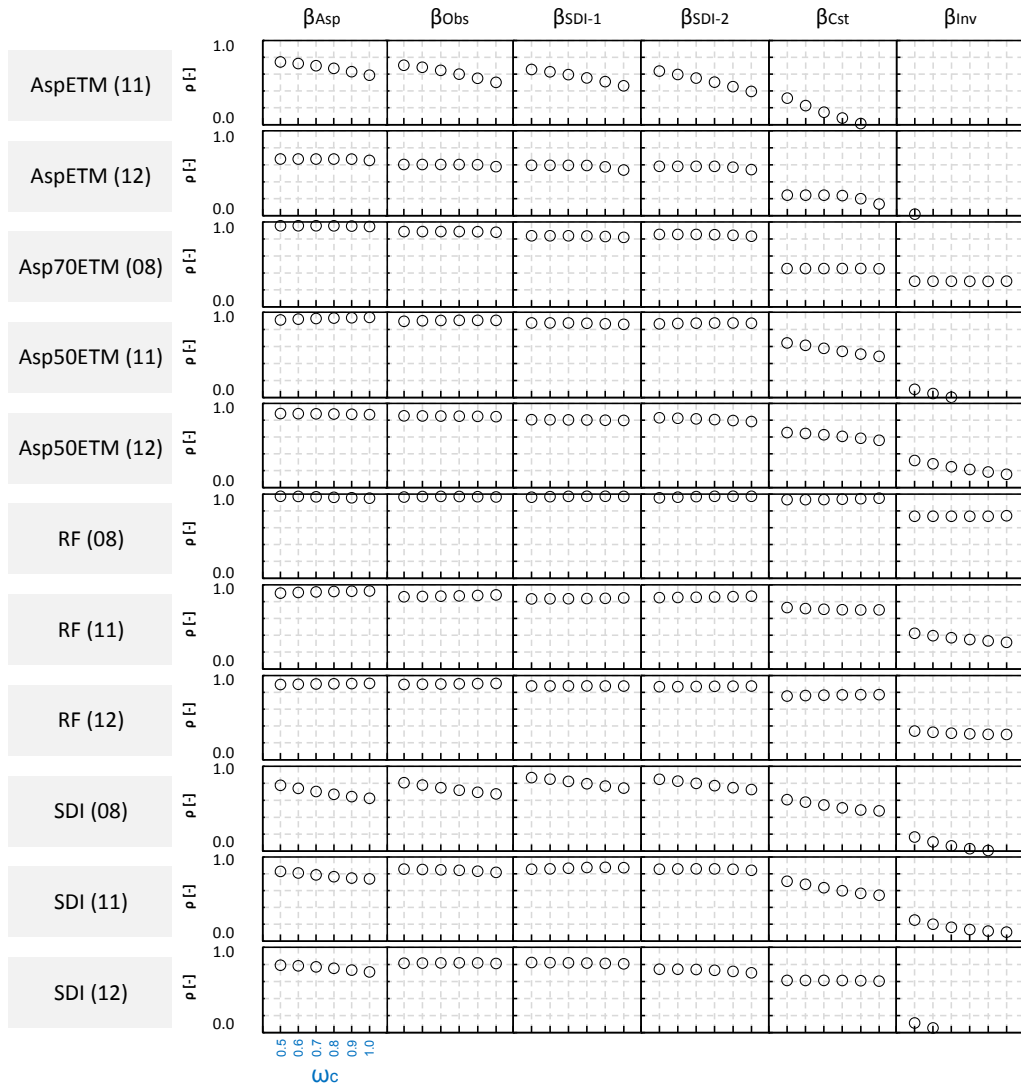


Figure 9: Correlation coefficient of Pearson (ρ) between θ_{obs} and θ_{sim} profiles for all scenarii. Only the positive ρ values are shown.

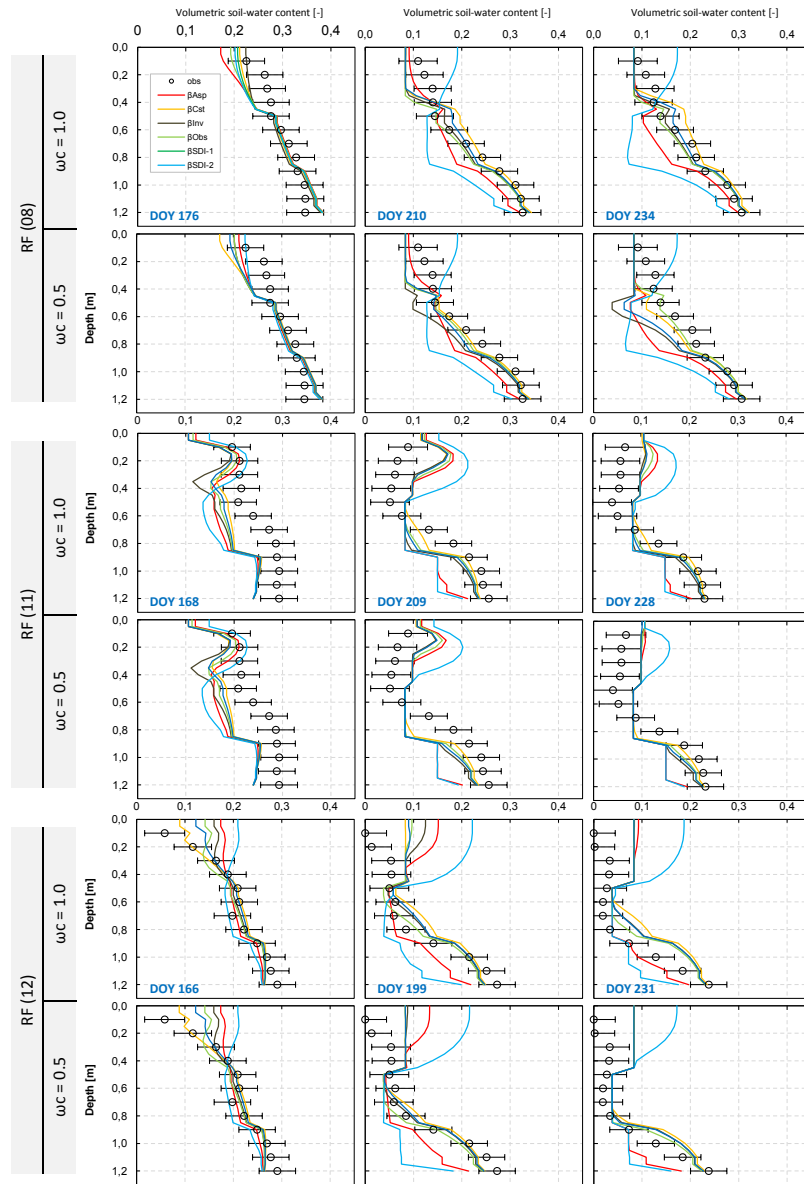


Figure 10: Comparison between θ_{sim} and θ_{obs} for all rainfed treatments, for non and maximum compensatory RWU level. The horizontal bars represent measurement errors corresponding to the neutron probe calibration equation.

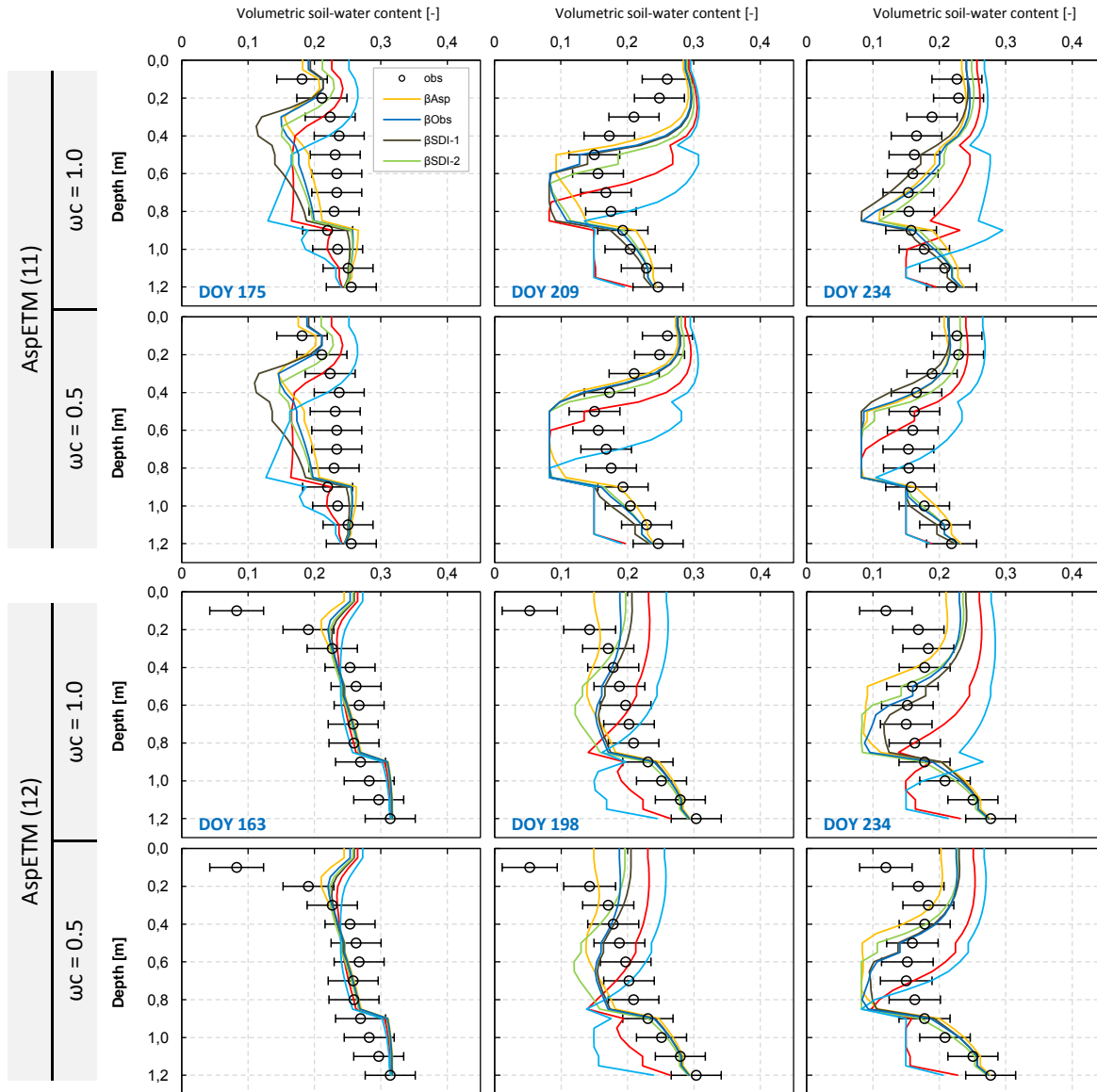


Figure 11: Comparison between θ_{sim} and θ_{obs} for the fully-irrigated sprinkler treatments, for non and maximum compensatory RWU level. The horizontal bars represent measurement errors corresponding to the neutron probe calibration equation.

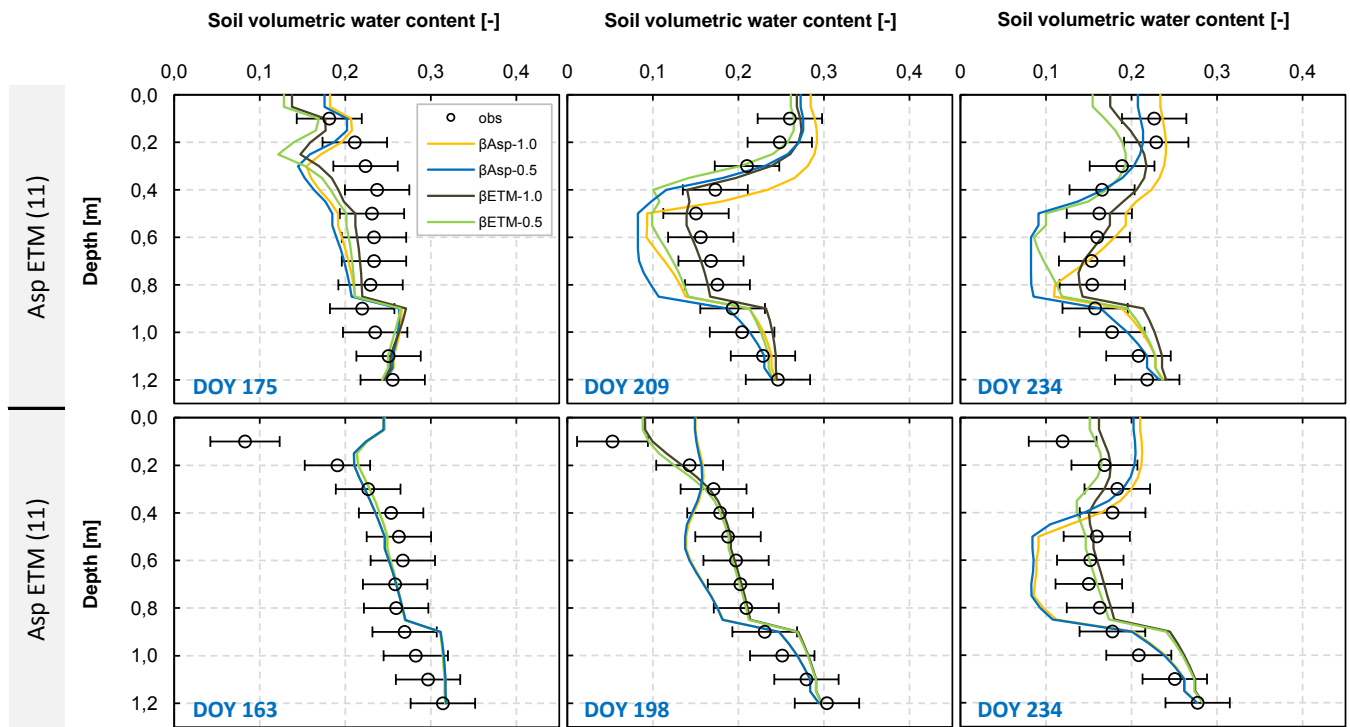


Figure 12: Comparison between θ_{sim} and θ_{obs} for the fully-irrigated treatments. The simulations were conducted using β_{Asp} and β_{ETM} profiles, for non and maximum compensatory RWU level. The horizontal bars represent measurement errors corresponding to the neutron probe calibration equation.

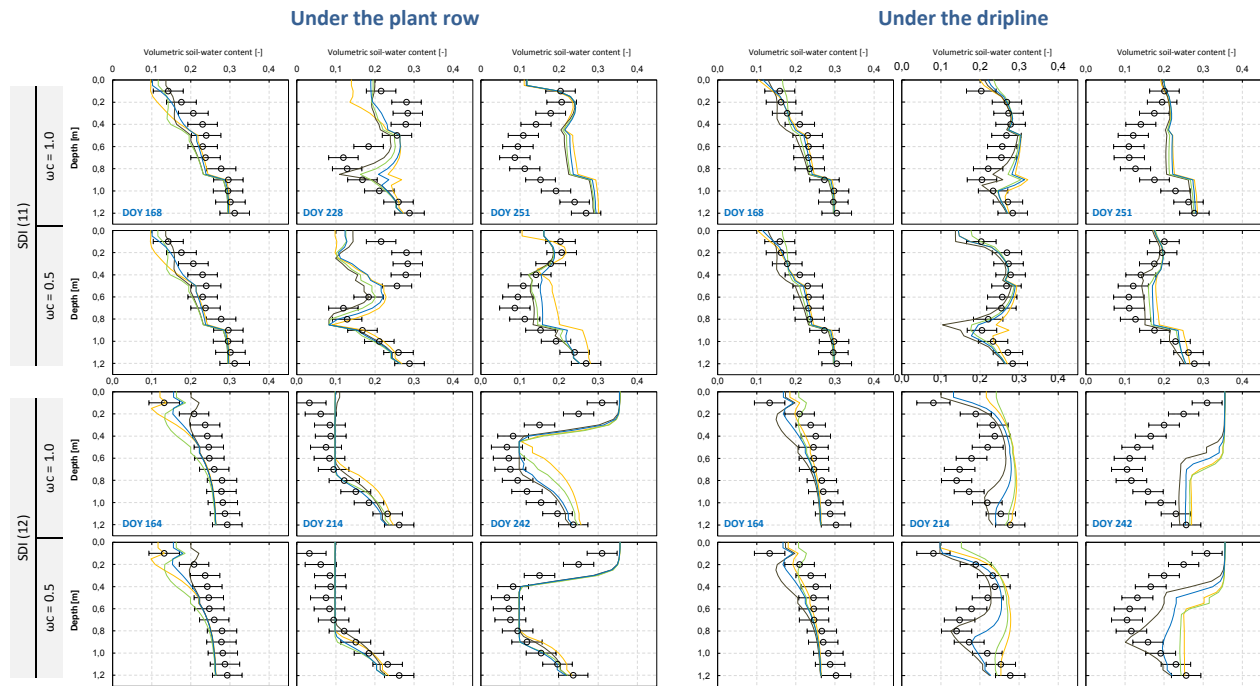


Figure 13: Comparison between θ_{sim} and θ_{obs} under plant row and in the vertical plane of the dripline for SDI (11) and SDI (12), for non and maximum compensatory RWU levels. The horizontal bars represent measurement errors corresponding to the neutron probe calibration equation.

Soil layer [cm]	clay (%)	silt (%)	sand (%)	θ_r [-]	θ_s [-]	α [cm^{-1}]	n [-]	Ks [cm day^{-1}]	l [-]	
0 - 55	55	18	42	40	0.00	0.36	0.0436	1.227	40.56	0.5
55 - >	90	22	47	31	0.05	0.38	0.013	1.45	12.00	0.5
>	90	25	52	18	0.09	0.41	0.019	1.31	6.19	0.5

Table 1: The hydrodynamic parameters of the van Genuchten (1980) model fitted to the soil of Lavalette station. θ_r and θ_s denote respectively the residual and saturated volumetric soil water contents, α and n are empirical shape parameters, Ks is the soil hydraulic conductivity at saturation and l is a pore connectivity parameter.

	All β profiles				“Realistic” β profiles (β_{Asp} , β_{Obs} , β_{SDI-1} and β_{SDI-2})			
	Non compensatory		Compensatory uptake		Non compensatory		Compensatory uptake	
	$\omega_c = 1.0$		$\omega_c = 0.5$		$\omega_c = 1.0$		$\omega_c = 0.5$	
	Max-Min [mm]	1-min/max (%)	Max-Min [mm]	1-min/max (%)	Max-Min [mm]	1-min/max (%)	Max-Min [mm]	1-min/max (%)
AspETM (11)	63	14.0	52	10.2	9	2.0	6	1.3
AspETM (12)	56	10.5	3	0.6	11	2.1	0	0.1
Asp70ETM (08)	22	4.5	0	0.0	11	2.4	0	0.0
Asp50ETM (11)	38	11.6	34	9.6	9	2.9	7	2.1
Asp50ETM (12)	36	10.7	28	8.0	10	3.3	5	1.5
RF (08)	87	34.1	33	12.6	28	14.5	15	6.4
RF (11)	28	15.4	27	14.0	6	3.7	8	4.4
RF (12)	59	23.3	35	13.0	16	7.5	9	3.8
SDI (08)	60	14.8	26	5.4	43	11.1	16	3.4
SDI (11)	50	12.0	17	3.6	37	9.2	10	2.2
SDI (12)	97	23.7	71	14.8	83	21.1	71	14.8

Table 2: The differences between the maximum and the minimum simulated cumulative transpiration $T_{a\ cum}$ for each treatment, using all β profiles (columns 2 to 5) and only those of the “realistic” group (columns 6 to 9).

	All β profiles		“Realistic” β profiles (β_{Asp} , β_{Obs} , $\beta_{\text{SDI-1}}$ and $\beta_{\text{SDI-2}}$)	
	Non compensatory	Compensatory uptake	Non compensatory	Compensatory uptake
	$\omega_c = 1.0$	$\omega_c = 0.5$	$\omega_c = 1.0$	$\omega_c = 0.5$
AspETM (11)	7	6	1	1
AspETM (12)	15	19	2	2
Asp70ETM (08)	36	37	6	6
Asp50ETM (11)	13	12	1	1
Asp50ETM (12)	16	16	2	2
RF (08)	24	19	5	3
RF (11)	5	5	1	1
RF (12)	15	15	2	2
SDI (08)	28	20	11	5
SDI (11)	17	13	5	3
SDI (12)	69	47	50	24

Table 3: The differences between the maximum and the minimum simulated cumulative drainage $\text{Drain}_{\text{cum}}$ outfluxes for each treatments, using all β profiles (columns 2 and 3) and only those of the “realistic” group (columns 4 and 5).

(a) non compensatory RWU	β_{Asp}	β_{Obs}	$\beta_{\text{SDI-1}}$	$\beta_{\text{SDI-2}}$	β_{Cst}	β_{Inv}
AspETM (11)	0.064 a	0.074 a b c	0.082 a b c	0.071 a b	0.082 b c	0.085 c
AspETM (12)	0.065 a b	0.062 a b	0.057 a	0.071 a b	0.071 a b	0.083 b
Asp70ETM (08)	0.039 a	0.043 a	0.048 a	0.049 a	0.078 b	0.086 b
Asp50ETM (11)	0.043 a	0.044 a	0.047 a	0.051 a	0.083 b	0.108 c
Asp50ETM (12)	0.055 a	0.060 a b	0.073 b c	0.061 a b	0.088 c d	0.101 d
RF (08)	0.049 a	0.047 a	0.045 a	0.051 a b	0.056 a b	0.082 a b
RF (11)	0.075 a	0.085 a b	0.092 b c	0.085 a b	0.108 c d	0.118 d
RF (12)	0.119 a	0.117 a	0.116 a	0.112 a	0.102 a	0.111 a
SDI (08)	0.061 a	0.054 a	0.053 a	0.054 a	0.062 a	0.081 b
SDI (11)	0.057 a	0.047 a	0.048 a	0.052 a	0.064 a	0.080 b
SDI (12)	0.055 a	0.053 a	0.048 a	0.067 a	0.083 b	0.113 c
(b) compensatory RWU						
AspETM (11)	0.081 a	0.083 a	0.092 a	0.082 a	0.089 a	0.088 a
AspETM (12)	0.067 a b	0.063 a b	0.060 a	0.072 a b	0.071 a b	0.084 b
Asp70ETM (08)	0.039 a	0.042 a	0.046 a	0.051 a	0.079 b	0.088 b
Asp50ETM (11)	0.054 a	0.055 a	0.056 a	0.063 a	0.084 a	0.105 b
Asp50ETM (12)	0.055 a	0.063 a b	0.075 b c	0.060 a b	0.089 c d	0.101 d
RF (08)	0.056 a	0.061 a	0.061 a b c	0.071 a	0.066 a	0.084 a
RF (11)	0.087 a	0.095 a b	0.100 a	0.094 a b	0.112 a b c	0.118 c
RF (12)	0.113 a	0.098 a	0.111 a	0.107 a	0.098 a	0.105 a
SDI (08)	0.063 a	0.056 a	0.064 a b	0.065 a b	0.070 a b	0.085 b
SDI (11)	0.072 a	0.070 a	0.079 a	0.081 a	0.077 a	0.082 a
SDI (12)	0.064 a	0.062 a b	0.050 a	0.074 b c	0.086 c d	0.106 d

Table 4: Root-mean-squared errors (RMSE) [-] between θ_{sim} and θ_{obs} profiles for non compensatory (a) and compensatory uptake (b) simulations. RMSE values followed by the same letters indicate no statistically significant differences ($\alpha = 0.5$).